The Numerical Approximation of Blow-Up Times for Fractional Reaction-Diffusion Equations

by

Mariam Khachatryan

A dissertation submitted to the Graduate Faculty of
Auburn University
in partial fulfillment of the
requirements for the Degree of
Doctor of Philosophy

Auburn, Alabama
August 6, 2022

Keywords: blow-up solution, fractional operator, numerical blow-up time

Approved by

Hans Werner van Wyk, Chair, Associate Professor of Mathematics and Statistics
Erkan Nane, Co-chair, Professor of Mathematics and Statistics
Yanzhao Cao, Professor of Mathematics and Statistics
Thi-Thao-Phuong Hoang, Assistant Professor of Mathematics and Statistics
Mark Dougherty, Associate Professor of Biosystems Engineering

Abstract

We investigate the numerical estimation of blow-up phenomena of the space fractional reaction-diffusion equation

$$\partial_t u + (-\Delta)^{\alpha/2} u = f(u), \quad x \in \Omega, t > 0$$

with non-negative initial and Dirichlet boundary conditions. First, we consider the full discretization of the fractional equation using the already existing novel and accurate finite difference method for the fractional operator. Next, we implement an auxiliary function H to the blow-up. The numerical blow-up times are computed for the fractional reaction-diffusion equation with the reaction term $f(u) = u^2$ and $f(u) = e^u$. Convergence results are proven. Moreover, the numerical blow-up time computed for the fractional reaction-diffusion equation with $\alpha \to 2$ is compared with the numerical blow-up time for the classical reaction-diffusion equation with $\alpha = 2$, and consistent results are obtained.

Acknowledgments

I express my gratitude to my advisors Dr. Hans-Werner van Wyk and Dr. Erkan Nane for their great patience and support in guiding me through this journey. I am sincerely thankful for all the help I have gotten. You indeed made my Ph.D. more enjoyable, and I can't thank you enough for all the skills I have learned from you. I am forever thankful for your encouragement, especially during my job search; I know how drastically it changed my perspective and boosted my confidence. This all would have been impossible without your continuous support and understanding. THANK YOU!

I thank my committee members, Dr. Yanzhao Cao, Dr. Thi Thao Phuong Hoang, and my University reader Dr. Mark Dougherty for their availability, support, and especially for their valuable comments and suggestions during my general oral exam.

Dr. Anahit Khacatryan and Dr. Michael Poghosyan from Yerevan State University helped me start this journey; for that, I am most grateful. My friends, colleagues, and, of course, professors from ICPT, Italy, set my path as a scientist and provided me with ample opportunities to succeed. I am overwhelmed with all the support and guidance I have received from my beloved department of Math and Stats at Auburn University. This is where I grew as a teacher and a researcher. Parker Hall indeed became home in the past years, and that's because of my amazing friends Dr. Maria Onyido, Dr. Meaza Bogale, Dr. Fauziya Yakasai, and Dr. Mark Uzochukwu. You all became an integral part of my life.

Lastly, I would like to thank my parents, Aram Khachatryan and Angela Sargsyan, who taught me to stay humble and focused. They showed me the importance of education. An immense thankfulness goes to my elder brother Dr. Hrachya Khachatryan who motivated me to start a Ph.D. and was my inspiration throughout.

Table of Contents

List of Figures

List of Tables

Chapter 1

Introduction

Reaction-diffusion equations model quantities that experience local concentration changes and are spread out in space. Applications range from chemical and biological processes [43, 41, 44] to medicine, genetics [24, 19, 29], physics, chemistry [47], social science, finance [8, 9], and weather prediction. For example, in applications to population biology [48, 50], the reaction term models growth, while the diffusion term explains migration. In the typical form of the reaction-diffusion equation

$$u_t = D\Delta u + f(u),$$

the solution $u(t, x)$ represents the population density or the concentration of the substance at time t and position x, Δ is the standard Laplace operator which describes the diffusion, D is the diffusion coefficient, and $f(u)$ is the reaction term.

Reaction-diffusion models can be studied under different growth models, i.e., exponential growth, logistic growth, and confined exponential growth. For exponential growth

$$f(u) = au,$$

where a is the growth rate, while in the logistic case

$$f(u) = au\Big(1 - \frac{u}{K}\Big),$$

where K is the carrying capacity.

The standard Laplace operator in semi-linear reaction-diffusion equations has been widely studied, whereas the non-local generalization remains not entirely examined. The

Laplace operator in R^n is

$$\Delta = \frac{\partial^2}{\partial x_1^2} + \frac{\partial^2}{\partial x_2^2} + ... + \frac{\partial^2}{\partial x_n^2}$$

which was introduced by Pierre-Simon Laplace and was used initially in the studies of celestial mechanics. Fractional Laplacian is a pseudo-differential operator that generalizes the notion of the standard Laplace operator $(-\Delta)$ to the Laplace operator with fractional powers. The fractional Laplace operator is denoted by $(-\Delta)^{\alpha/2}$.

Recent research studies suggest that the classical diffusion equation is insufficient in modeling many real-world situations, where a particle plume propagates more quickly than that predicted by the classical model. The system may exhibit significant asymmetry called anomalous diffusion. A popular model for anomalous diffusion is fractional diffusion, where a fractional derivative of order less than two is used instead of the classical second derivative in space. So, for systems exhibiting anomalous diffusion [10, 51, 20], the diffusive spread is commonly modeled by a non-local fractional Laplace operator $(-\Delta)^{\alpha/2}$ with fractional exponent $\alpha \in (0, 2]$. This gives rise to the following space-fractional partial differential equation

$$\partial_t u + (-\Delta)^{\alpha/2} u = f(u), \tag{1.1}$$

where $f(u)$ is a non-negative source term. The phenomenon of finite-time blow-up is present in such models. The solution u of Equation (1.1) is said to blow up at finite time T if $u \to \infty$ as $t \to T^-$.

For $\alpha = 2$ the fractional operator $(-\Delta)^{\alpha/2}$ simplifies to the standard Laplace operator $(-\Delta)$ and the equation (1.1) simplifies to the following standard reaction-diffusion equation

$$u_t - u_{xx} = f(u), \quad x \in \Omega \subset R^n, t > 0. \tag{1.2}$$

The theoretical properties, as well as the time and space discretization of Equation (1.2), have been intensively studied previously. In particular, [18] provides a complete discretization scheme for studying problems such as (1.2) for $f(u) = u^p$. The finite difference method presented in [18, 17] is the generalization of the work in [49]. Nakagawa [49] considered a finite difference scheme for the special case of Equation (1.2) when the

reaction term is $f(u) = u^2$. Moreover, it is known that under certain initial and boundary conditions, the solution blows up in finite time (i.e., the solution becomes unbounded in finite time). However, the blow-up phenomena of the space-fractional reaction-diffusion equation remains partially understood.

The critical exponents for blow-ups of the reaction-diffusion equation with anomalous diffusion

$$\begin{aligned} \partial_t u + (-\Delta)^{\alpha/2} u = \lambda u^p, \quad x \in R^n, t > 0 \\ u(x,0) = u_0(x) > 0 \end{aligned} \tag{1.3}$$

where $\alpha \in (0, 2]$ and $\lambda \in \{-1, 1\}$, have been studied in [25]. The Equation (1.3) with standard Laplace operator has been studied by many authors, namely Fujita [26] has shown

$$\begin{cases} \text{for any initial condition no global positive solution exists} & \text{if} \quad p < 1 + 2/N \\ \text{for small initial data global solutions exist} & \text{if} \quad p > 1 + 2/N \end{cases}$$

The proof for the critical case $p = 1 + 2/N$, which results in blow-up solutions, can be found in [30, 40, 55], The paper [25] discusses and proves analogous results but for the fractional Laplace operator. One of their findings which is of great interest to us is for Equation (1.3) with $\lambda = 1$ where the re-scaled test function is used to prove the blow-up of all positive solutions when $p = 1 + \alpha/N$. The finite time blow-up for the critical exponent $p < 1 + \alpha/N$ has been studied and proved previously in [28, 27]. The findings related to the fractional Laplace operator in the papers mentioned above are in line with the numerical blow-up results obtained in this thesis.

Typical questions to be asked when working with differential equations with possible blow-up solutions are

- Is there a blow-up?
- When does it occur?
- Where does it occur?

- How is it detected numerically?

This thesis investigates the blow-up phenomena of fractional partial differential equations (FPDEs), namely the fractional reaction-diffusion equation. Some standard ordinary differential equations (ODE) and partial differential equations (PDE) blow-up results are presented in Chapter 1. The fully discretized scheme of Equation (2.1) is provided in Section 2.1.2, where the fractional Laplace operator is discretized based on the trapezoidal rule introduced in [23]. In Chapter 2, we perform convergence analysis and provide several error estimate results. The adapted numerical algorithm with an auxiliary function H is applied to the blow-up problem described in Section 2.1. The blow-up times are estimated numerically for the proposed FPDEs. Comparison of blow-up time for FPDE ($\alpha \to 2$) and PDE ($\alpha = 2$) is provided in Section 2.3 and consistent blow-up times are obtained. Concluding remarks are followed in Section 2.4.

1.1 Standard Results - ODE Blow-Up

The simplest differential equations to be studied in the context of blow-ups are the ordinary differential equations. Consider the following first-order nonlinear differential equation with $m > 1$

$$u'(t) = u^m, \quad t > 0 \tag{1.4}$$

with the initial value $u(0) = u_0 > 0$. As the solution is explicitly given by

$$u(t) = \frac{u_0}{(1-(m-1)u_0^{m-1}t)^{1/m-1}},$$

we notice that the blow-up happens at

$$T = \frac{1}{(m-1)u_0^{m-1}}.$$

If we define the numerical blow-up time to be $T(\tau) = \tau n_\tau$ and $U_0 = u_0$ then from the work of Cho [18] it is known that

$$-\int_{H^{-1}(\frac{1}{\tau})}^{\infty} \frac{ds}{f(s)} \leq T(\tau) - T \leq -\int_{H^{-1}(\frac{1}{\tau})}^{\infty} \frac{ds}{f(s)} + \tau\Big(1 + \ln \frac{f(H^{-1}(\frac{1}{\tau})}{f(U_0)}\Big).$$

$H : [0, \infty) \to [0, \infty)$ is a monotone increasing function that satisfies the following two conditions

$$H(s) > 0 \quad \text{for} \quad s > 0 \quad \text{and} \quad \lim_{s\to\infty} H(s) = \infty.$$

To illustrate the blow-up and show the possible problem associated with it, we consider a special case of Equation (1.4)

$$u'(t) = u^2, \quad t > 0 \tag{1.5}$$

with the initial value

$$u(0) = u_0 > 0.$$

The solution is given by

$$u(t) = \frac{u_0}{1 - u_0 t}$$

which clearly has a pole (also known as blow-up) at time

$$T = 1/u_0.$$

Consider the following initial condition $u_0 = 1$. To get the numerical solution of Equation (1.5) we implement a forward Euler scheme. We discretize the ODE and the initial condition as follows

$$\frac{U^{n+1} - U^n}{\Delta t_n} = (U^n)^2$$

with

$$U^0 = 1$$

$t_0 = 0$, $t_n = \sum_{j=1}^{n-1} \Delta t_j$ are the nodal points. Next, we plot the exact solution and the numerical solution for $\Delta t_n = 0.02$ and $\Delta t_n = 0.05$.

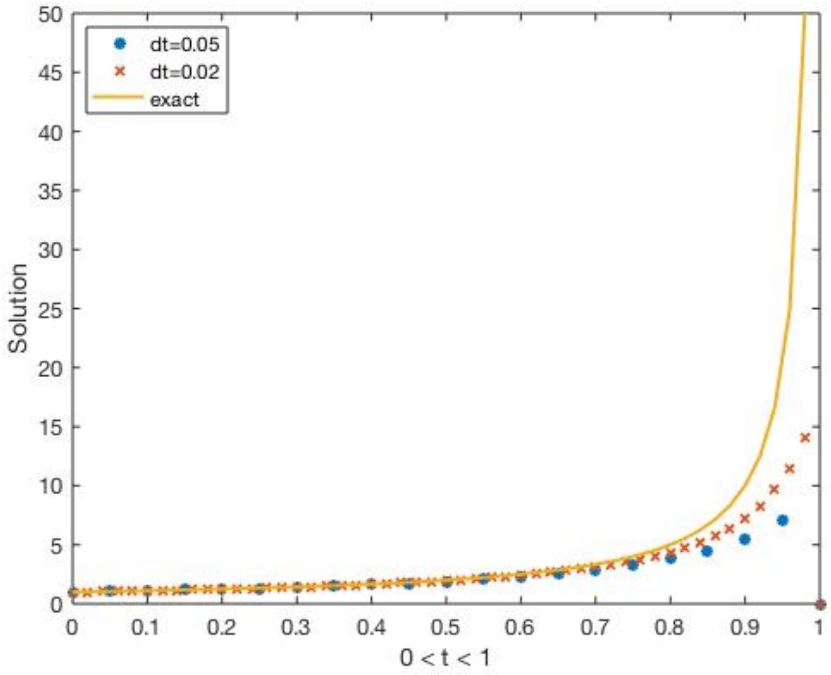

Figure 1.1: Exact and numerical solutions of (1.5), forward Euler with the step-size 0.02 and 0.05.

We notice the numerical solutions approach the exact solution as the step size gets smaller; however, the numerical scheme misses the blow-up time, $t = 1$. Hence, a different scheme is required as long as the blow-up is concerned.

1.2 Standard Results - PDE Blow-Up

Studying the blow-up phenomena is more challenging when working with partial differential equations. One of the well-studied yet actual cases is the semi-linear heat equation given in (1.2). The blow-up phenomena of Equation (1.2) has been studied with the Dirichlet boundary condition

$$u(0,t) = u(1,t) = 0 \quad x \in \partial\Omega.$$

f is a smooth enough function, in particular, is a C^1 (continuously differentiable) function. It is also known that under appropriate growth conditions imposed on function f, the solution blows up in finite time. Motivated by paper [18] as a preliminary result we discretize Equation (1.2) with the following initial condition $u_0 = 100\sin(\pi x)$ where $x \in (0, 1)$ to detect the blow-time. The estimated numerical blow-up time is $T_1 = 0.010800$. See Figure 1.2. In the following scheme the $H(s) = s$ and the stability condition

$$\lambda = \frac{\Delta t}{(dx)^2} \leq \frac{1}{2}$$

is satisfied. It is worth mentioning that different choices of the H function and the norms will result in different blow-up times and hence different accuracy.

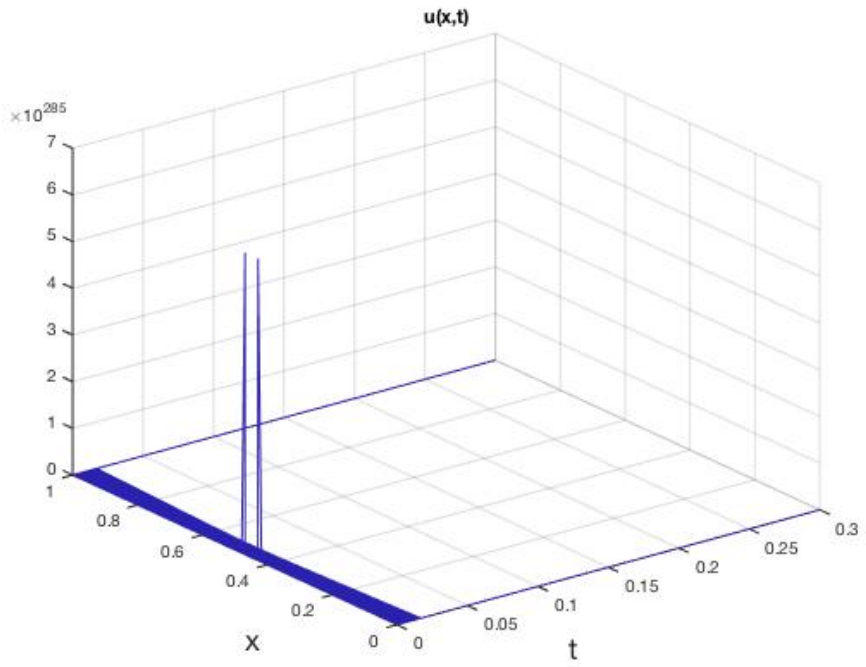

Figure 1.2: Numerical blow-up estimate of equation (1.2) with $f(u) = u^2$ and $u_0 = 100\sin(\pi x)$ where u_t is discretized by forward Euler scheme and central difference scheme is used for u_{xx}.

Similar results are also present in the following papers of Cho [18], and Nakagawa [49]. The main concerns that various authors have addressed, including Chen [16] and Nakagawa [49] are

- how to estimate the blow-up time numerically using a finite difference scheme such that it will not miss the blow-up time
- how well the numerical scheme will reproduce it.

Chapter 2

Space-Fractional Reaction-Diffusion Equation

2.1 Problem Setting

The following fractional reaction-diffusion equation is studied in this thesis

$$\begin{aligned} \partial_t u + (-\Delta)^{\alpha/2} u &= f(u), \quad x \in \Omega, t > 0 \\ u(x,0) &= u_0(x) \geq 0, \quad x \in \Omega \\ u(x,t) &= 0, \quad x \in \Omega^c, t > 0. \end{aligned} \tag{2.1}$$

We aim to

- estimate the blow-up time numerically for the following reaction terms

$$f(u) = u^2 \quad \text{and} \quad f(u) = e^u$$

  under appropriate initial conditions that will be specified in Section 2.3 when the numerical experiments are performed.

- adapt and use a numerical scheme that will detect the blow-up time.

- generalize the convergence and error estimate results in [18] from PDE to FPDE case.

- compute the numerical blow-up time for the fractional reaction-diffusion equation when $\alpha \to 2$ to compare with the numerical blow-up time for the standard reaction-diffusion equation when $\alpha = 2$.

2.1.1 Fractional Laplace Operator

Marcel Riesz was one of the first to initiate the study of the fractional Laplace operator [53]. Since the operator can be used to describe different phenomena and has various applications, numerous definitions have been proposed as a result. The numerical schemes used to discretize the fractional Laplace operator also vary depending on its representation. For example, a specific numerical strategy was discussed in [2]. The numerical scheme in [2] for solving fractional reaction-diffusion is based on matrix transfer techniques (MTT) that was originally introduced in [36] and [6]. The fractional Laplace operator can be defined as a pseudo-differential operator using the Fourier transform

$$(-\Delta)^{\alpha/2}u(\mathbf{x}) = \mathcal{F}^{-1}[|k|^{\alpha}\mathcal{F}[u]], \tag{2.2}$$

for $\alpha > 0$. $\mathcal{F}$ and $\mathcal{F}^{-1}$ are the Fourier and Inverse Fourier transforms, respectively. The standard Laplace operator is a special case of (2.2) for $\alpha = 2$.

If $u : R^n \to R$, then the fractional Laplacian defined in terms of the hypersingular integral is given by

$$(-\Delta)^{\alpha/2}u(\mathbf{x}) = c_{n,\alpha}P.V.\int_{R^n}\frac{u(\mathbf{x}) - u(\mathbf{y})}{|\mathbf{x}-\mathbf{y}|^{n+\alpha}}d\mathbf{y} \tag{2.3}$$

for $\alpha \in (0, 2)$, and the $c_{n,\alpha}$ is a constant given by

$$c_{n,\alpha} = \frac{2^{\alpha-1}\alpha\Gamma(\frac{\alpha+n}{2})}{\sqrt{\pi^n}\Gamma(1-\frac{\alpha}{2})}$$

where P.V. stands for the Cauchy principal value and Γ represents the Gamma function. There are other equivalent representations of the fractional Laplace operator, such as

- Balakrishna's definition

$$(-\Delta)^{\alpha/2}u(x) = \frac{\sin\left(\pi\frac{\alpha}{2}\right)}{\pi}\int_0^{\infty}(-\Delta)\big(t-\Delta\big)^{-1}u(x)\frac{dt}{t^{1-\alpha/2}}$$

- the spectral fractional Laplacian of u

$$(-\Delta)^{\alpha/2}u(x) = \frac{1}{\Gamma(-\alpha/2)}\int_0^\infty (e^{t\Delta}u(x) - u(x))\frac{dt}{t^{1+\alpha/2}}$$

  where $e^{t\Delta}$ is heat semigroup.

- as the generator of α-stable Lévy processes

$$(-\Delta)^{\alpha/2}u(x) = \lim_{h\to 0^+}\frac{1}{h}E[u(x) - u(x + X_h)]$$

  where X_t is the isotropic α-stable Lévy process.

For a complete list of representations of the fractional Laplace operator, refer to [42, 21]. In this thesis, we will use the one-dimensional fractional Laplace operator written in terms of the hypersingular integral

$$(-\Delta)^{\alpha/2}u(x) = c_{1,\alpha}P.V.\int_R \frac{u(x) - u(y)}{|x - y|^{1+\alpha}}dy \tag{2.4}$$

for $\alpha \in (0, 2)$, and the $c_{1,\alpha}$ is a constant given by

$$c_{1,\alpha} = \frac{2^{\alpha-1}\alpha\Gamma(\frac{\alpha+n}{2})}{\sqrt{\pi}\Gamma(1 - \frac{\alpha}{2})}$$

where P.V. stands for the Cauchy principal value and Γ represents the Gamma function.

2.1.2 Discretization of the Fractional Laplace Operator

The discretization of Laplacian in (2.2) when $\alpha = 2$ has been thoroughly examined; however, the numerical methods for the fractional case are still being discussed. There are many challenges; one is the numerical approximation of (2.3) with higher accuracy.

We will be using the numerical scheme introduced in [23] where the weighted trapezoidal rule (WTR) is used to approximate the fractional Laplacian given in (2.3) after formulating it as a weighted integral of a weaker singular function on the bounded domain $\Omega = (-l, l)$. The physical domain $\Omega = (-l, l)$ of width $L = 2l$ is subdivided into

K sub-intervals of equal width $h = L/K$ with grid points $\{x_i\}_{i=0}^K$ given by $x_i = -l + ih$ for $i = 0, \ldots, K$. For any grid function $\{U_i\}_{i=0}^K$, whose value in Ω^c is U_∞, the discrete fractional Laplacian is

$$
\begin{aligned}
-(-\Delta)_h^{\alpha/2} U_j = \frac{c_{1,\alpha}}{2} \Bigg(& \delta_\gamma^1 U_j \int_0^h \xi^{\gamma-(\alpha+1)} d\xi \\
& + \sum_{k=2}^{K} \frac{c_{1,\alpha}}{2} \left(\delta_\gamma^{k-1} U_j + \delta_\gamma^k U_j \right) \int_{\xi_{k-1}}^{\xi_k} \xi^{\gamma-(\alpha+1)} d\xi \\
& + 2c_{1,\alpha}(U_j - U_\infty) \int_L^\infty \xi^{-(1+\alpha)} d\xi \Bigg), \quad (2.5)
\end{aligned}
$$

where

$$\delta_\gamma^k U_j = \frac{U_{j+k} - 2U_j + U_{j-k}}{(kh)^\gamma}.$$

Denote the discretized fractional Laplacian by $\mathcal{L}_{h,\alpha} := -(-\Delta)_h^{\alpha/2} u(x_j, t_n)$. The finite difference scheme of (2.3) in matrix notation is given by

$$(-\Delta)_{h,\gamma}^{\alpha/2} \mathbf{u} = A\mathbf{u}$$

where $\gamma \in (\alpha, 2]$ is the introduced splitting parameter. A is the matrix representation of the fractional Laplacian given by

$$
A_{ij} = C_{\alpha,\gamma}^h \begin{cases} \sum_{k=2}^{K-1} \frac{(k+1)^\nu - (k-1)^\nu}{k^\gamma} + \frac{K^\nu - (K-1)^\nu}{K^\gamma} + (2^\nu + k_\gamma - 1) + \frac{2\nu}{\alpha K^\alpha} & \text{for } j = i \\ -\dfrac{(|j-i|+1)^\nu - (|j-i|-1)^\nu}{2|j-i|^\gamma}, & \text{for } j \neq i, i \pm 1 \\ -\dfrac{1}{2}(2^\nu + k_\gamma - 1), & \text{for } j = i \pm 1. \end{cases} \quad (2.6)
$$

where

$$C_{\alpha,\gamma}^h = \frac{c_{1,\alpha}}{\nu h^\alpha}$$

and $\nu = \gamma - \alpha$. The matrix representation 2.6 for $\alpha = 2$ simplifies to central difference scheme discussed in [18]

$$\frac{U_j^{n+1} - U_j^n}{\Delta t_n} - \frac{U_{j+1}^n - 2U_j^n + U_{j-1}^n}{h^2} = f(U_j^n).$$

This will also be tested numerically. The finite difference equation for Problem (2.1) is thus given by

$$\frac{U_j^{n+1} - U_j^n}{\tau} + (-\Delta)_h^{\alpha/2} U_j^n = f(U_j^n), \qquad j = 1, \ldots, K-1, n = 1, \ldots. \tag{2.7}$$

Equation (2.7) yields the explicit updating rule

$$U_j^{n+1} = (I - \tau(-\Delta)_h^{\alpha/2}) U_j^n + \tau f(U_j^n). \tag{2.8}$$

For convenience, we define $L = (I - \tau(-\Delta)_h^{\alpha/2})$ so that $U_j^{n+1} = LU_j^n + .\tau f(U_j^n)$.

Let $H : [0, \infty) \to [0, \infty)$ be a monotone increasing function that satisfies

$$H(s) > 0 \text{ for } s > 0 \qquad \text{and } \lim_{s \to \infty} H(s) = \infty.$$

We define our numerical approximation $\hat{T}$ of the blow-up time $T > 0$ to be the first time instant $\tau_n = n\tau$ so that

$$\tau_{n-1} H(\|U^{n-1}\|_\infty) < 1, \qquad \text{and } \tau_n H(\|U^n\|_\infty \geq 1. \tag{2.9}$$

2.2 Error Estimates and Convergence Analysis

In this section we prove stability and convergence of the finite difference scheme (2.7) before the blow-up time is reached, show that the finite difference solution is strictly increasing under conditions on f and u_0, and finally prove that the estimate (2.9) converges to the true blow-up time when τ and h tend to zero.

Assumption 1. Assume the reaction function $f : [0, \infty) \to \mathbb{R}$ appearing in the reaction-diffusion Equation (2.1) is positive, increasing, and convex, i.e. $f(u), f'(u), f''(u) > 0$ for all $u > 0$. Moreover, assume that the blow-up time exists, i.e.

$$T^* = \int_{U^0}^{\infty} \frac{1}{f(s)} ds < \infty. \tag{2.10}$$

We first establish a suitable α-dependent Courant-Friedrichs-Lewy (CFL) condition on the spatial and temporal discretization parameters, τ and h, that ensures stability of the forward Euler scheme (2.7).

Lemma 1. *For any $K \in \mathbb{N}$, $\alpha \in (0, 2)$, and $\nu = 2 - \alpha$,*

$$\sum_{k=2}^{K} \frac{(k+1)^\nu - (k-1)^\nu}{k^2} + \frac{K^\nu - (K-1)^\nu}{K^2} + \frac{2\nu}{\alpha K^\alpha} \leq \frac{2\nu}{\alpha}. \tag{2.11}$$

Proof. We attain this bound by noting that the upper bound in (2.11) is equal to the integral $2\int_1^\infty x^{-2} d(x^\nu)$, and that the sum on its left represents an underestimating numerical quadrature rule. Specifically, for any $k \geq 2$,

$$\frac{(k+1)^\nu - (k-1)^\nu}{k^2} = \int_{k-1}^{k+1} k^{-2} d(x^\nu) \approx \int_{k-1}^{k+1} x^{-2} d(x^\nu)$$

represents a weighted midpoint rule, whose error is given by

$$\int_{k-1}^{k+1} (x^{-2} - k^{-2}) d(x^\nu) = \int_{k-1}^{k+1} \nu (x^{-2} - k^{-2}) x^{\nu-1} dx.$$

If $\nu - 1 < 0$, the mapping $x \mapsto x^{\nu-1}$ is decreasing. This, together with the convexity of $x \mapsto x^{-2}$, then imply

$$\begin{aligned} \int_{k-1}^{k+1} \nu (x^{-2} - k^{-2}) x^{\nu-1} dx &\geq \nu (k+1)^{\nu-1} \int_{k-1}^{k+1} (x^{-2} - k^{-2}) dx \\ &\geq \nu (k+1)^{\nu-1} \int_{k-1}^{k+1} (-2k^{-3}(x-k)) dx = 0. \end{aligned} \tag{2.12}$$

If, on the other hand, $\nu - 1 > 0$, then it can readily be seen that the function $x \mapsto \nu x^{\nu-1}(x^{-2} - k^{-2})$ is decreasing, convex and has a zero at $x = k$. Similarly, the last term represents a weighted right-hand sum. If $\nu > 1$, then since $x \mapsto x^{-2}$ is decreasing,

$$\int_{K-1}^{K} (x^{-2} - K^{-2}) d(x^{\nu}) \geq 0,$$

whereas if $\nu < 1$, the differential $d(x^{\nu}) = \nu x^{\nu-1} dx$ is decreasing and hence

$$\begin{aligned} \int_{K-1}^{K} (x^{-2} - K^{-2}) d(x^{\nu}) &= \int_{K-1}^{K} (x^{-2} - K^{-2}) \nu x^{\nu-1} dx \\ &\geq \nu K^{\nu-1} \int_{K-1}^{K} (x^{-2} - K^{-2}) dx \geq 0. \end{aligned} \tag{2.13}$$

Estimates (2.12) and (2.13) now imply

$$\begin{aligned} &\sum_{k=2}^{K} \frac{(k+1)^{\nu} - (k-1)^{\nu}}{k^2} + \frac{K^{\nu} - (K-1)^{\nu}}{K^2} + \frac{2\nu}{\alpha K^{\alpha}} \\ \leq &\sum_{k=2}^{K} \int_{k-1}^{k+1} x^{-2} d(x^{\nu}) + \int_{K-1}^{K} x^{-2} d(x^{\nu}) + 2 \int_{K}^{\infty} x^{-2} d(x^{\nu}) \\ \leq &2 \int_{1}^{\infty} x^{-2} d(x^{\nu}) = \frac{2\nu}{\alpha}. \end{aligned}$$

□

Lemma 2. *If, for any $\eta \in (0, 1)$, the discretization parameters h and τ satisfy the CFL condition*

$$\frac{\tau}{h^{\alpha}} \leq \left(\frac{c_{1,\alpha}}{\nu} \left[\frac{2\nu}{\alpha} + 2^{\nu} + 1 \right] \right)^{-1} \eta, \tag{2.14}$$

then the diagonal entries of the matrix $L = I - \tau(-\Delta)_h^{\alpha/2}$ satisfy $L_{ii} \geq 1 - \eta$ for $i = 1, \ldots, K$. In this case, its induced maximum norm satisfies $\|L\|_{\infty} \leq 1$.

Proof. By virtue of the upper bound (2.11), we have

$$\tau \left[(-\Delta)_h^{\alpha/2} \right]_{ii} \leq \frac{\tau}{h^{\alpha}} \frac{c_{1,\alpha}}{\nu} \left[\frac{2\nu}{\alpha} + 2^{\nu} + 1 \right].$$

To establish a lower bound on the diagonal term L_{ii}, it thus suffices to show that the expression

$$s(\alpha) := \frac{c_{1,\alpha}}{\nu}\left[\frac{2\nu}{\alpha} + 2^{\nu} + 1\right] = \frac{2^{\alpha}\Gamma\left(\frac{1+\alpha}{2}\right)}{\sqrt{\pi}\Gamma\left(1-\frac{\alpha}{2}\right)} + \frac{2^{\alpha-1}\alpha\Gamma\left(\frac{1+\alpha}{2}\right)}{\nu\sqrt{\pi}\Gamma\left(1-\frac{\alpha}{2}\right)}(2^{\nu}+1)$$

is positive and bounded above for all $\alpha \in [0, 2]$. Clearly, $s(\alpha)$ is continuous and positive for $\alpha \in (0, 2)$, since it is a composition of continuous, positive functions on this domain. Using the fact that $\Gamma\left(\frac{1}{2}\right) = \sqrt{\pi}$, we obtain

$$\lim_{\alpha \to 0^+} s(\alpha) = 1.$$

Moreover, since $\nu\Gamma(1-\frac{\alpha}{2}) = 2\frac{\nu}{2}\Gamma(\frac{\nu}{2}) = 2\Gamma(1+\frac{\nu}{2})$, we have

$$\lim_{\alpha \to 2^-} \frac{2^{\alpha-1}\alpha\Gamma\left(\frac{1+\alpha}{2}\right)}{\nu\sqrt{\pi}\Gamma\left(1-\frac{\alpha}{2}\right)} = \lim_{\alpha \to 2^-} \frac{2^{\alpha-1}\alpha\Gamma\left(\frac{1+\alpha}{2}\right)}{\sqrt{\pi}2\Gamma\left(1+\frac{\nu}{2})\right)} = 1,$$

and since $\Gamma(\frac{\nu}{2}) \to \infty$ as $\alpha \to 2^-$ and hence $\nu \to 0^+$, we have

$$\lim_{\alpha \to 2^-} \frac{2^{\alpha}\Gamma\left(\frac{1+\alpha}{2}\right)}{\sqrt{\pi}\Gamma\left(1-\frac{\alpha}{2}\right)} = 0.$$

Combining these two limits yields

$$\lim_{\alpha \to 2^-} s(\alpha) = 2.$$

If τ and h are chosen to satisfy Inequality (2.14), then

$$L_{ii} = 1 - \tau\left[(-\Delta)_h^{\alpha/2}\right]_{ii} \geq 1 - \frac{\tau}{h^{\alpha}}s(\alpha) \geq 1 - \eta.$$

To bound $\|L\|_\infty$, we note that the CFL condition (2.14) guarantees $L_{ii} > 0$. Moreover, for $j = 1, ..., K-1$ and $j \neq i$, the off-diagonal terms

$$L_{ij} = -\tau \left[(-\Delta)_h^{\alpha/2}\right]_{ij} = \begin{cases} \frac{\tau}{h^\alpha}\frac{c_{1,\alpha}}{2\nu}(2^\nu + 1), & \text{if } j = i \pm 1 \\ \frac{\tau}{h^\alpha}\frac{c_{1,\alpha}}{2\nu}\left[\frac{(|j-i|+1)^\nu - (|j-i|-1)^\nu}{|j-i|^2}\right], & \text{if } |j-i| > 1 \end{cases}$$

are also nonnegative. Hence, the matrix norm is given by the maximum row sum, i.e.

$$\|L\|_\infty = \max_i \sum_{j=1}^{K-1} L_{ij} = 1 + \sum_{j=1}^{K-1} -\tau \left[(-\Delta)_h^{\alpha/2}\right]_{ij}.$$

We will show that $\sum_{j=1}^{K-1} -\tau \left[(-\Delta)_h^{\alpha/2}\right]_{ij} \leq 0$ for any $i = 1, ..., K-1$, from which the result follows. Indeed, letting $k = |i-j|$, we note that

$$\begin{aligned} \sum_{\substack{j=1 \\ |j-i|>1}}^{K-1} -\tau \left[(-\Delta)_h^{\alpha/2}\right]_{ij} &= \frac{\tau}{h^\alpha}\frac{c_{1,\alpha}}{2\nu} \sum_{\substack{j=1 \\ |j-i|>1}}^{K-1} \left[\frac{(|j-i|+1)^\nu - (|j-i|-1)^\nu}{|j-i|^2}\right] \\ &\leq \frac{\tau}{h^\alpha}\frac{c_{1,\alpha}}{\nu} \sum_{k=2}^{K-1} \left[\frac{(k+1)^\nu - (k-1)^\nu}{k^2}\right]. \end{aligned}$$

Also,

$$-\tau \left[(-\Delta)_h^{\alpha/2}\right]_{i,i-1} - \tau \left[(-\Delta)_h^{\alpha/2}\right]_{i,i+1} = \frac{\tau}{h^\alpha}\frac{c_{1,\alpha}}{\nu}(2^\nu + 1).$$

On the other hand,

$$\begin{aligned} -\tau \left[(-\Delta)_h^{\alpha/2}\right]_{ii} = \frac{\tau}{h^\alpha}\frac{c_{1,\alpha}}{\nu} \Bigg[&- \sum_{k=2}^{K-1} \frac{(k+1)^\nu - (k-1)^\nu}{k^2} - \frac{K^\nu - (K-1)^\nu}{K^2} \\ &-(2^\nu + 1) - \frac{2\nu}{\alpha K^\alpha}\Bigg]. \end{aligned}$$

Therefore,

$$\sum_{j=1}^{K-1} -\tau \left[(-\Delta)_h^{\alpha/2}\right]_{ij} \leq \frac{\tau}{h^\alpha}\frac{c_{1,\alpha}}{\nu} \left[-\frac{K^\nu - (K-1)^\nu}{K^2} - \frac{2\nu}{\alpha K^\alpha}\right] \leq 0.$$

□

Remark 1. Note that, since $s(\alpha) \to 2$ as $\alpha \to 2^-$, Inequality (2.14) reduces to the CFL condition

$$\frac{\tau}{h^2} \leq \frac{1}{2}\eta, \qquad \text{for } \eta \in (0,1),$$

which is used to ensure stability for the classical central difference scheme.

It follows from Theorem 3.2 in [23] and simple Taylor expansion arguments that the local truncation error $\zeta(\tau, h)$ of the scheme in (2.7), given by

$$\zeta(\tau,h) := \frac{u(x_j,t_{n+1}) - u(x_j,t_n)}{\tau} + (-\Delta)_h^{\alpha/2} u(x_j,t_n) - f(u(x_j,t_n)), \tag{2.15}$$

satisfies $\zeta(\tau, h) = O(\tau + h^2)$ as $\tau, h \to 0^+$, provided the solution $u \in C^2([0,T], C^{3,\alpha}(\Omega))$ for any time $T < T^*$ before the blow-up. The global convergence before onset of the blow-up now follows by standard arguments. Specifically

Theorem 2.1. Let the error $E^n \in \mathbb{R}^{K-1}$ be given by $E_j^n = u(x_j, t_n) - U_j^n$, for $j = 1, \dots K-1$ and $n = 1, ..., N$, and for any time $t_N < T^*$, let

$$C = \max_{\substack{0<t<t_N \\ x\in\Omega}} |f'(u(x,t))|.$$

Then, for any $\tau > 0$ and $h > 0$ satisfying the CFL condition (2.14), we have

$$\|E^N\|_\infty \leq \frac{e^{Ct_N}}{C}\left(C\|E^0\|_\infty + \zeta(\tau,h)\right) = O(\tau + h^2). \tag{2.16}$$

Proof. Applying the updating formula (2.8) to the error and invoking Equation (2.15) gives

$$E_j^N = LE_j^{N-1} + \tau\left[f(u(x_j,t_{N-1})) - f(U_j^{N-1})\right] + \tau\zeta(\tau,h),$$

We proceed to bound $\|E^N\|_\infty$ recursively, making use of geometric series and the bound $\|L\|_\infty \leq 1$ under Condition (2.14), to obtain

$$\begin{aligned}
\|E^N\|_\infty &\leq (1+\tau C)\|E^{N-1}\|_\infty + \tau\zeta(\tau,h) \\
&\leq (1+\tau C)^N\|E^0\|_\infty + \tau\zeta(\tau,h)\sum_{n=0}^{N-1}(1+\tau C)^n \\
&= (1+\tau C)^N\|E^0\|_\infty + \left(\frac{(1+\tau C)^N-1}{C}\right)\zeta(\tau,h) \\
&\leq \frac{(1+\tau C)^N}{C}\left(C\|E^0\|_\infty + \zeta(\tau,h)\right).
\end{aligned}$$

The result now follows from the inequality $(1+\tau C)^N \leq e^{N\cdot\tau C} = e^{Ct_N}$. □

2.2.1 Existence and Error of Numerical Blow-Up Time

In this section we show that for a sufficiently large initial condition, the finite difference approximation U_j^n diverges as $n \to \infty$ so that the numerical blow-up estimate given in (2.9) is well-defined. Specifically, we make the following assumption.

Assumption 2. Assume that the initial condition $U^0 \geq 0$ satisfies

$$-(-\Delta)_h^{\alpha/2}U_i^0 + f(U_i^0) \geq af(U_i^0),\ i = 0,\ldots,K, \tag{2.17}$$

for some $a \in (0,1)$, where $U_i^0 = u_0(x_i)$ for $i = 0,\ldots K$.

Lemma 3. *For the function f satisfying Assumptions 1 and 2 and any grid function U_i on Ω that is constant on Ω^c, we have*

$$(-\Delta)_h^{\alpha/2}f(U_i) \leq f'(U_i)(-\Delta)_h^{\alpha/2}U_i, \qquad i = 1,...,K-1. \tag{2.18}$$

Proof. Applying a first order Taylor approximation to the central difference and using the convexity of f, we obtain

$$\begin{aligned}\delta_2^k f(U_i) &= \frac{f(U_{i+k}) - 2f(U_i) + f(U_{i-k})}{\xi_k^2} \\ &= f'(U_i)\delta_2^k U_i + \frac{f''(\zeta_1)}{2\xi_k^2}(U_{i+k} - U_i)^2 + \frac{f''(\zeta_2)}{2\xi_k^2}(U_{i-k} - U_i)^2 \\ &\geq f'(U_i)\delta_2^k U_i,\end{aligned}$$

where ζ_1 is some point between U_i and U_{i+k} and ζ_2 lies between U_i and U_{i-k}. Similarly,

$$f(U_i) - f(U_\infty) \geq f'(U_i)(U_i - U_\infty).$$

The result now follows from the definition of the discrete fractional Laplacian given in terms of central differences by Equation (2.5). □

The following lemma shows that under the above assumptions, the finite difference solution is increasing with time and hence there exists an approximate blow up time.

Lemma 4. *Let U_j^n solve the finite difference equation* (2.7) *and Assumptions 1 and 2 hold, then*

$$\frac{U_i^{n+1} - U_i^n}{\tau} = -(-\Delta)_h^{\alpha/2} U_i^n + f(U_i^n) \geq a f(U_i^n), \tag{2.19}$$

for any $i = 1, ..., K-1$, and $n \geq 1$.

Proof. Let

$$V_i^n = -(-\Delta)_h^{\alpha/2} U_i^n + (1-a) f(U_i^n),$$

for $i = 1, \ldots, K-1$ and $n \geq 1$. By Assumption 2, $V_i^0 \geq 0$ for $i = 1, \ldots K-1$. Suppose by way of induction that $V_i^n \geq 0$ for $i = 1, \ldots, K-1$. Then, by definition

$$\frac{V_i^{n+1} - V_i^n}{\tau} = \mathcal{L}_{h,\alpha}\left(\frac{U_i^{n+1} - U_i^n}{\tau}\right) + (1-a)\left(\frac{f(U_i^{n+1}) - f(U_i^n)}{\tau}\right). \tag{2.20}$$

Using the finite difference Equation (2.7) and Lemma 3 gives

$$\begin{aligned}\mathcal{L}_{h,\alpha}\left(\frac{U_i^{n+1}-U_i^n}{\tau}\right) &= \mathcal{L}_{h,\alpha}(\mathcal{L}_{h,\alpha}U_i^n + f(U_i^n)) \\ &\geq \mathcal{L}_{h,\alpha}V_i^n + af'(U_i^n)\mathcal{L}_{h,\alpha}U_i^n.\end{aligned}$$

Moreover, using Taylor expansion in conjunction with the convexity of f and Equation (2.7) yields

$$\begin{aligned}\left(\frac{f(U_i^{n+1})-f(U_i^n)}{\tau}\right) &= f'(U_i^n)\left(\frac{U_i^{n+1}-U_i^n}{\tau}\right) + \frac{f''(\zeta_i^n)}{2\tau}\left(U_i^{n+1}-U_i^n\right)^2 \\ &\geq f'(U_i^n)\left(\mathcal{L}_{h,\alpha}U_i^n + f(U_i^n)\right),\end{aligned}$$

where ζ_i^n is some point between U_i^n and U_i^{n+1}. Combining these two estimates in Equation (2.20) gives

$$\begin{aligned}\frac{V_i^{n+1}-V_i^n}{\tau} &\geq \mathcal{L}_{h,\alpha}V_i^n + af'(U_i^n)\mathcal{L}_{h,\alpha}U_i^n + (1-a)f'(U_i^n)\left(\mathcal{L}_{h,\alpha}U_i^n + f(U_i^n)\right) \\ &= \mathcal{L}_{h,\alpha}V_i^n + f'(U_i^n)V_i^n \geq \mathcal{L}_{h,\alpha}V_i^n,\end{aligned}$$

by the positive slope of f and the induction hypothesis. To prove $V_i^{n+1} \geq 0$ for $i = 1, \ldots, K-1$, it suffices to show that $(I + \tau\mathcal{L}_{h,\alpha})V_i^n \geq 0$. This in turn is only possible if *all* entries of $I + \tau\mathcal{L}_{h,\alpha}$ are non-negative. Moreover, Expression (2.10) in [23] reveals that all off-diagonal entries in $\mathcal{L}_{h,\alpha}$ are non-negative, and by Lemma 2 the diagonal entries are also non-negative. □

Lemma 5. *If (2.19) then*

$$\frac{\|U^{n+1}\|_\infty - \|U^n\|_\infty}{\tau} \geq af(||U^n||_\infty) \tag{2.21}$$

Proof. From

$$\frac{U_j^{n+1}-U_j^n}{\tau} \geq af(U_j^n)$$

where

$$\|U_j^n\|_\infty = \max_j |U_j^n|$$

$$U_j^{n+1} \geq \tau a f(U_j^n) + U_j^n$$

$$\|U_j^{n+1}\|_\infty \geq \tau a f(U_j^n) + U_j^n$$

Specifically, $U_{\tilde{j}}^n = ||U^n||_\infty$ for $j = \tilde{j}$

$$\|U_j^{n+1}\|_\infty \geq \tau a f(\|U^n\|_\infty) + \|U^n\|_\infty$$

□

Consequence of (2.21)

$$\lim_{n\to\infty} U_j^n = \infty$$

$$\sum_{n=0}^{N} \frac{||U^{n+1}||_\infty - ||U^n||_\infty}{\tau} = \frac{||U^{n+1}||_\infty - ||U^0||_\infty}{\tau}$$
$$\geq a \sum_{n=0}^{N} f(||U^n||_\infty) \to \infty \quad \text{as} \quad N \to \infty$$

This means that a numerical stopping time exists. For any H with $H(s) > 0$, $H'(s) > 0$ for some s and $\lim_{s\to\infty} H(s) = \infty$ there is n_τ such that

$$\tau H(||U^{n_\tau - 1}||_\infty < 1, \quad \tau H(||U^{n_\tau}||_\infty \geq 1.$$

Use Proposition 2 in [1] with condition

$$\sigma^2 U_j^0 + f(U_j^0) \geq 0$$

replaced with

$$-(-\Delta)_h^{\alpha/2} U_j^0 + (1-a) f(U_j^0) \geq 0 \quad \text{for some } a \in (0,1).$$

Recall that the L^p norm is defined by

$$\|U^n\|_p = \begin{cases} \left(\sum_{j=1}^{N-1} h |U_j^n|^p \right)^{\frac{1}{p}}, & \text{if } 1 \leq p < \infty \\ \max_{j=1,\dots N-1} |U_j^n|, & \text{if } p = \infty \end{cases}$$

Definition 1. Let T be the blow-up time of the solution u of Equation (2.1). Define $T_\infty = \tau n_\tau$ to be the numerical blow-up time.

Theorem 2.2. If H satisfies

$$\tau \ln f\Big(H^{-1}\Big(\frac{1}{\tau}\Big)\Big) \to 0 \quad \text{as} \quad \tau \to 0,$$

then $T_\infty \to T$ as $\tau \to 0$.

Proof. We omit the proof of the theorem as it is essentially proved in the following papers of Nakagawa [49] and Cho [18, 17]. □

2.3 Numerical Experiments

In this section, we apply the discretization scheme described in Section 2.1.2 for the fractional Laplace operator $-(-\Delta)^{\alpha/2}$. We aim to detect and estimate the numerical blow-up times for Problem (2.1), in particular when the reaction term is $f(u) = u^2$ and $f(u) = e^u$, verify error estimates and convergence results numerically.

2.3.1 The Blow-up Time for the Reaction Term $f(u) = u^2$

Example 1. Consider the equation $\partial_t u + (-\Delta)^{\alpha/2} u = u^2, x \in \Omega = (-1,1), t > 0$ with the following non-negative initial condition

$$u(0,x) = u_0 = \begin{cases} 7(1-x^2)^{1+m} & x \in (-1,1) \\ 0 & else \end{cases}$$

and the zero Dirichlet boundary condition

$$u(x,t) = 0 \quad x \in R \setminus \Omega, t > 0.$$

We should choose an increasing function $H(s)$ such that $\lim_{s\to\infty} H(s) = \infty$ and

$$\tau \ln f\Big(H^{-1}\Big(\frac{1}{\tau}\Big)\Big) \to 0 \quad \text{as} \quad \tau \to 0,$$

for $\tau > 0$. We stop the numerical computation when $H(||U^{n_\tau}||_\infty \geq 1$ at the step n_τ. There is no well ordered way to choose the function H. However, following [22] we will begin with $H(s) = s$ as a starting choice. The discrete initial and boundary conditions are

$$U_j^0 = u_0(x_j), \quad j = 1, ..., J-1$$

and

$$U_0^n = U_J^n = 0 \quad n \geq 0,$$

where h is the spatial grid size and τ is the temporal mesh size.

Similar to the classical Laplace operator, the stability condition needs to be ensured for the fractional case since explicit methods have been used. We have previously shown that *all* entries of $I + \tau\mathcal{L}_{h,\alpha}$ are non-negative. Now, we aim to find an estimate for C. This will also help us to establish our numerical results and ensure the stability of the scheme. We start with

$$1 - \tau\frac{c_{1,\alpha}}{\nu h^\alpha}\left(\sum_{k=2}^{K-1}\frac{(k+1)^\nu - (k-1)^\nu}{k^\gamma} + \frac{K^\nu - (K-1)^\nu}{K^\gamma} + 2^\nu + \kappa_\gamma - 1 + \frac{2\nu}{\alpha K^\alpha}\right) \geq 0.$$

Equivalently,

$$\tau\frac{c_{1,\alpha}}{\nu h^\alpha}\left(\sum_{k=2}^{K-1}\frac{(k+1)^\nu - (k-1)^\nu}{k^\gamma} + \frac{K^\nu - (K-1)^\nu}{K^\gamma} + 2^\nu + \kappa_\gamma - 1 + \frac{2\nu}{\alpha K^\alpha}\right) \leq 1.$$

We need to find an upper bound C

$$\sum_{k=2}^{K-1} \frac{(k+1)^\nu - (k-1)^\nu}{k^\gamma} + \frac{K^\nu - (K-1)^\nu}{K^\gamma} + 2^\nu + \kappa_\gamma - 1 + \frac{2\nu}{\alpha K^\alpha} \leq C, \tag{2.22}$$

where C does not depend on h (or K), then we can ensure positivity by choosing

$$\tau \leq \frac{\nu}{C c_{1,\alpha}} h^\alpha.$$

We have that

$$\begin{aligned}
\gamma &\in (\alpha, 2], \\
\nu &= \gamma - \alpha, \\
K &= \frac{L}{h}, \\
\kappa_\gamma &= \begin{cases} 1, & \text{if } \gamma \in (\alpha, 2) \\ 2, & \text{if } \gamma = 2 \end{cases} \\
c_{1,\alpha} &= \frac{2^{\alpha-1}\alpha\Gamma((\alpha+1)/2)}{\sqrt{\pi}\Gamma(1-\alpha/2)}
\end{aligned}$$

The Tables 2.1 and 2.2 estimate the expression (2.22) for different values of α, γ and κ_γ.

Table 2.1: Estimating expression (2.22) for $\kappa_\gamma = 2$

α	1	0.5	1.5	1.999
γ	2	2	2	2
$\nu = \gamma - \alpha$	1	1.5	0.5	0.001
estimate	**4.290**	**8.649**	**2.763**	**2.001**

Table 2.2: Estimating expression (2.22) for $\kappa_\gamma = 1$

α	0.5	0.5	0.5	1.5
γ	0.5	1	1.5	1.999
$\nu = \gamma - \alpha$	0	0.5	1	0.499
estimate	**1.000**	**3.044**	**5.225**	**1.762**

We use estimate C to ensure the stability

$$\lambda = \frac{\tau}{h^\alpha} \leq \frac{\nu}{C c_{1,\alpha}}.$$

Table 2.3: Stability when $\kappa_\gamma = 2$

α	γ	ν	C	λ
0.1	2	1.9	41.142	0.9749
0.3	2	1.7	14.199	0.9232
0.5	2	1.5	8.649	0.8695
0.7	2	1.3	6.193	0.8145
0.9	2	1.1	4.790	0.7595
1	2	1	4.290	0.7323
1.3	2	0.7	3.236	0.6537
1.5	2	0.5	2.763	0.6048
1.999	**2**	**0.001**	**2.001**	**0.5002**

Table 2.4: Stability when $\kappa_\gamma = 1$

α	γ	ν	C	λ
0.1	0.5	0.4	9.012	0.9369
0.3	1	0.7	5.744	0.9396
0.5	0.5	0	1	0
0.5	1	0.5	3.044	0.8235
0.5	1.5	1	5.225	0.9595
0.7	1	0.3	1.878	0.6199
0.7	1.5	0.8	3.435	0.9036
1.5	1.999	0.499	1.762	0.9465
1.7	1.999	0.299	1.400	0.9564

From Table 2.3 when $\alpha = 1.999$ the stability condition is $\lambda = 0.5002$ which is close to the stability in the standard case. This is expected theoretically as for $\alpha = 2$ the weighted trapezoidal rule simplifies to the central difference scheme, which has the stability condition $\lambda \leq 0.5$.

When $\alpha = 1.5, \gamma = 2$ the fractional equation with the specified parameters

$$\begin{aligned} L &= 2l = 2, \\ K &= 100, \\ h &= \frac{L}{K} = \frac{1}{50}, \\ \tau &= \frac{0.3}{50^2} \end{aligned}$$

leads to the following λ

$$\lambda = \frac{\tau}{h^\alpha} = \frac{0.3}{50^2} \cdot 50^{1.5} \approx 0.0431$$

which is less than the estimated upper bound 0.6048. Hence, the stability is ensured.

Next, we need to compute the blow-up time for the fractional PDE. The estimated numerical blow-up time for the specified parameters is $T_\infty = 0.209880$. See Figure 2.1 below.

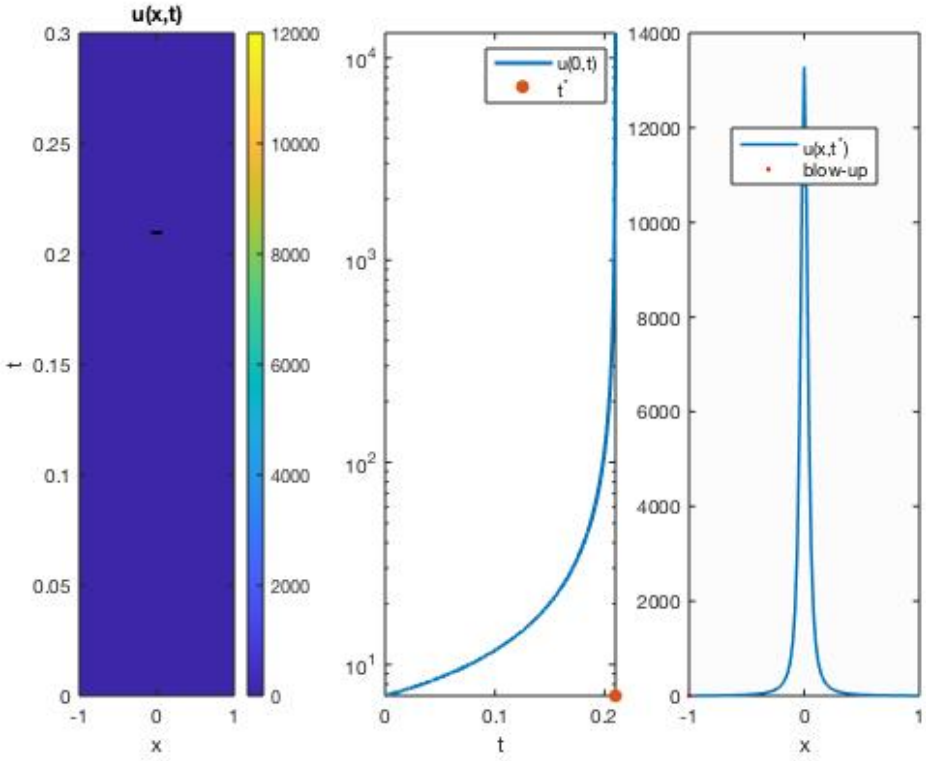

Figure 2.1: $\partial_t u + (-\Delta)^{\alpha/2} u = u^2, x \in (-1, 1)$, with $\alpha = 1.5$, $T_\infty = 0.209880$

As mentioned before, different choices of function H and different norms will lead to different numerical blow-up times. It is very difficult to observe a systematic way of choosing the function H. Our choice of H is the identity $H(s) = s$. The table below shows blow-up times for different choices of H. We observe that the blow-up times are different by an amount that is within the following range $(0.00012, 0.00648)$.

Table 2.5: T_∞ and T_1 numerical blow-up times for $\partial_t u + (-\Delta)^{\alpha/2} u = u^2, x \in (-1,1), \alpha = 1.5$.

$H(s) = s^m$	T_∞	T_1
m=0.5	0.210360	0.210480
m=1	0.209880	0.210120
m=1.1	0.209640	0.210120
m=1.3	0.208800	0.209880
m=4/3	0.208560	0.209880
m=3/2	0.207120	0.209400
m=1.7	0.204360	0.208200
m=1.9	0.200160	0.205800
m=2	0.197520	0.204000

This table suggests a pattern which we illustrate graphically below. The convergence is from below for large H while the convergence is from above for small H. See Figure 2.2.

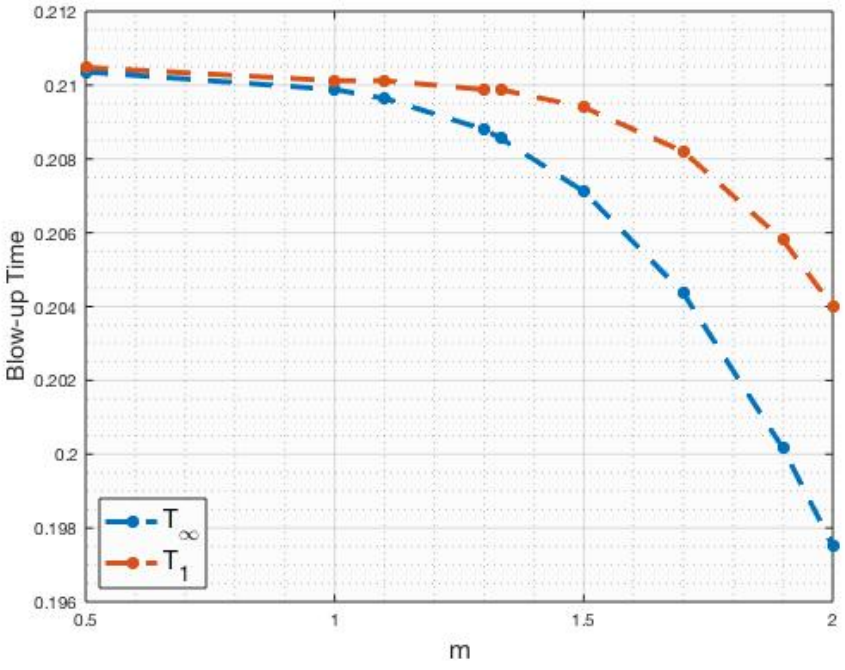

Figure 2.2: T_∞ and T_1 blow-up times for different choices of H.

However, we aim to find an optimal H numerically. The reference blow-up time corresponding to $nt = 2^{19}$ is $T_\infty = 0.209056$ and is $T_1 = 0.209058$. Next we estimate the error to find what H will minimize the error. The error is defined as

$$\text{error} = |\text{ reference blow-up time - blow-up time}|.$$

We find that for T_∞ the error is minimized when $m = 1.3$ and for T_1 when $m = 1.5$. We illustrate that graphically. See Figure 2.3.

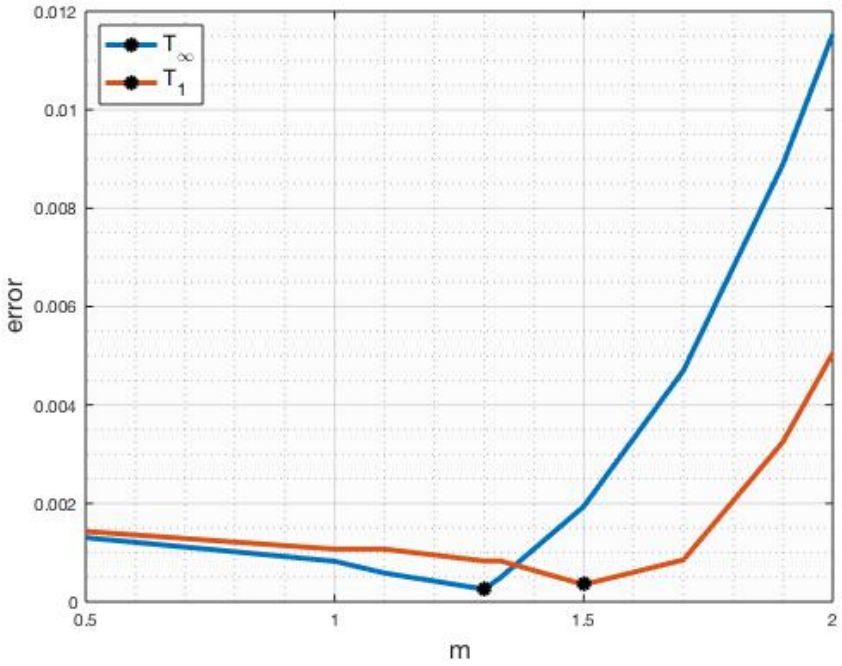

Figure 2.3: The error for different choices of H.

Next, we set the splitting parameter $\gamma = 2$ and compute the blow-up times for different choices of α. The table below suggests a pattern. We observe that the blow-up happens at a later time when α gets larger. We also notice that the T_∞ and T_1 blow-up times are different as it was expected, and the difference is within the following range $(0.00024, 0.00036)$.

Table 2.6: T_∞ and T_1 for $\partial_t u + (-\Delta)^{\alpha/2} u = u^2, x \in (-1,1), \gamma = 2, H(s) = s$.

α	T_∞	T_1
0.3	0.157800	0.158160
0.5	0.161040	0.161400
0.8	0.168480	0.168840
1	0.176280	0.176640
1.3	0.193920	0.194160
1.5	0.209880	0.210120
1.7	0.228840	0.229200
1.9	0.251040	0.251280
1.999	0.263760	0.264000

The plot below is the illustration of Table 2.6.

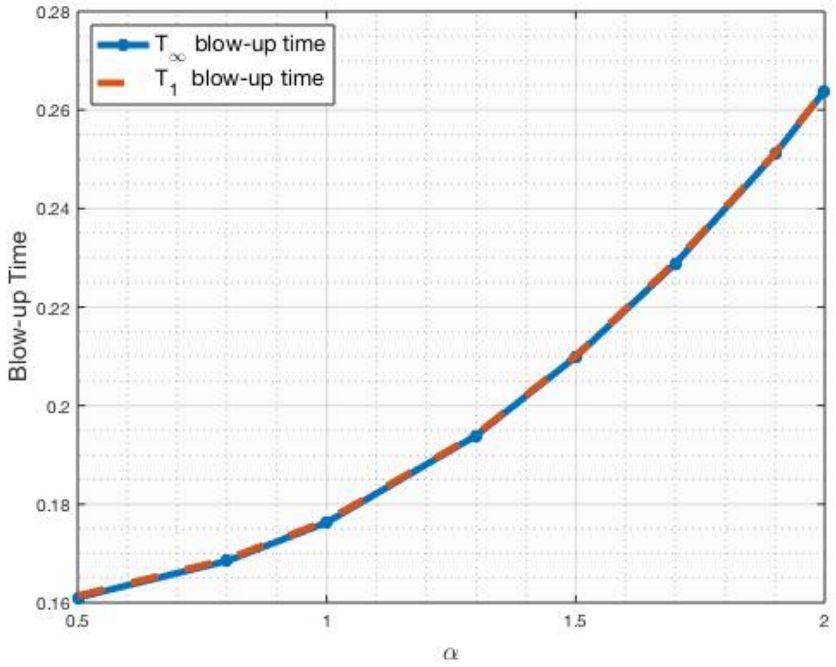

Figure 2.4: T_∞ and T_1 blow-up times using $\alpha \in [0.3, 1.999]$.

Next, we numerically estimate the T_1 blow-up time. When $\alpha = 1.5$ and the $H(s) = s$ the estimated blow-up time is $T_1 = 0.210120$.

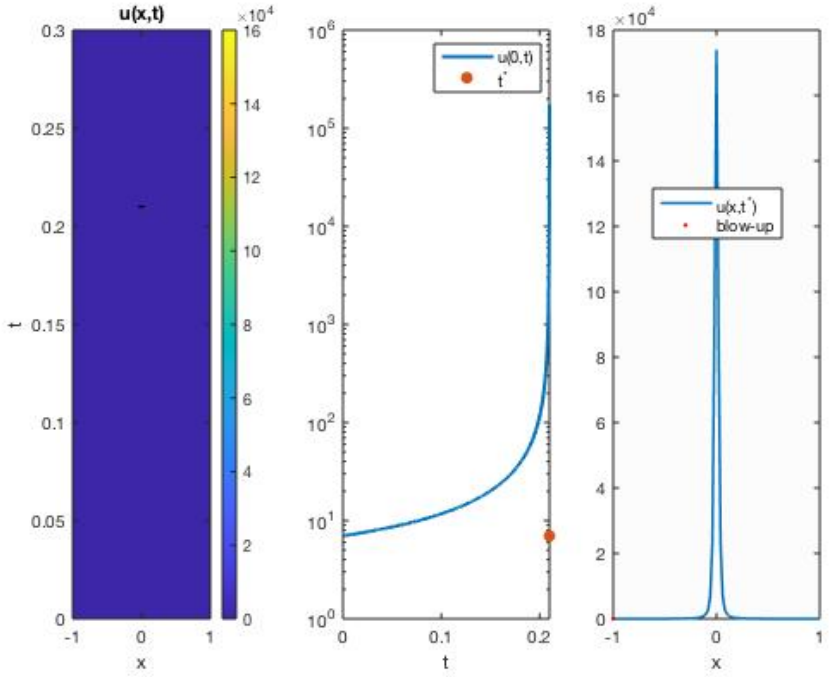

Figure 2.5: $\partial_t u + (-\Delta)^{\alpha/2} u = u^2, x \in (-1,1)$, with $\alpha = 1.5$, $T_1 = 0.210120$.

Below two different blow-up situation are illustrated for $H(s) = s^2$ and $\alpha = 1.5$, $H(s) = \sqrt{s}$ and $\alpha = 1.5$. The estimated numerical blow-up times are $T_\infty = 0.197520$ and $T_\infty = 0.210360$, respectively.

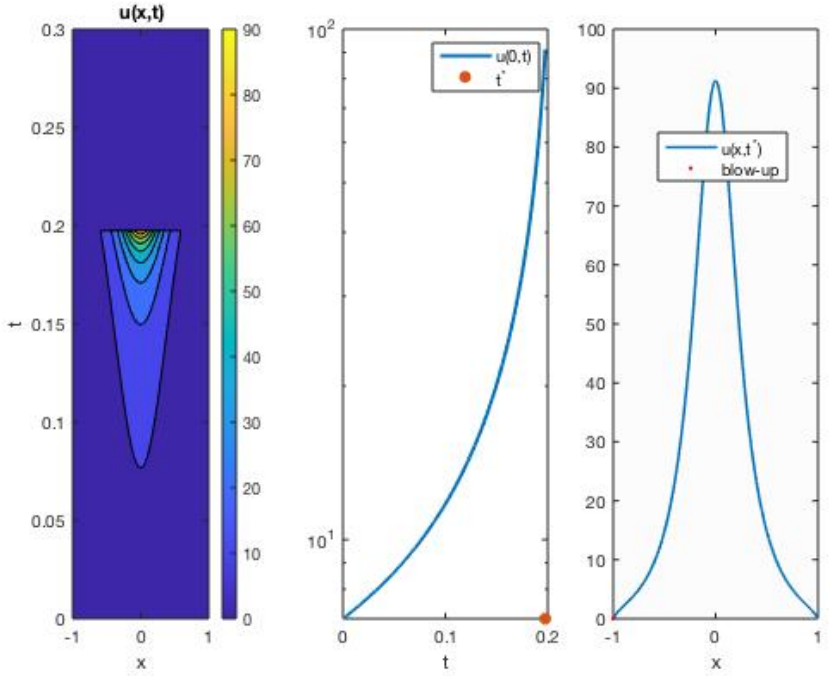

Figure 2.6: $\partial_t u + (-\Delta)^{\alpha/2} u = u^2, x \in (-1,1)$, $\alpha = 1.5, H(s) = s^2$, $T_\infty = 0.197520$.

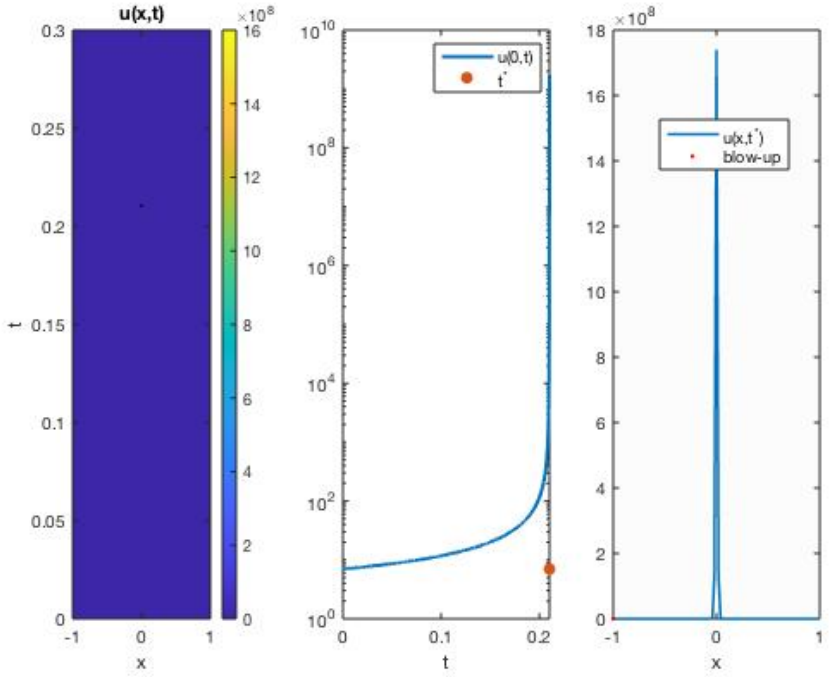

Figure 2.7: $\partial_t u + (-\Delta)^{\alpha/2} u = u^2, x \in (-1,1)$, $\alpha = 1.5, H(s) = \sqrt{s}$, $T_\infty = 0.210480$.

2.3.2 The Blow-up Time for the Reaction Term $f(u) = e^u$

Example 2. Consider the following fractional equation

$$\partial_t u + (-\Delta)^{\alpha/2} u = e^u, x \in \Omega = (-1,1), t > 0$$

with the exponential reaction term and with the following non-negative initial condition

$$u(0,x) = u_0 = \begin{cases} 3(1-x^2)^{1+m} & x \in (-1,1) \\ 0 & else \end{cases}$$

and the zero Dirichlet boundary condition

$$u(x,t) = 0 \quad x \in R \setminus \Omega, t > 0.$$

We apply the same discretization described previously in Section 2.1.2. We choose a non-negative increasing function $H(s) = e^s - 1$ to help to detect the numerical blow-up time. The estimated blow-up time is $T_\infty = 0.083040$ when $\alpha = 1.5$. Moreover, since

$T_1 = 0.083520$ we will omit the graph. We observe the blow-up happens at an earlier time compared to $f(u) = u^2$. Also, notice that the initial condition is not taken as large as it is for $f(u) = u^2$.

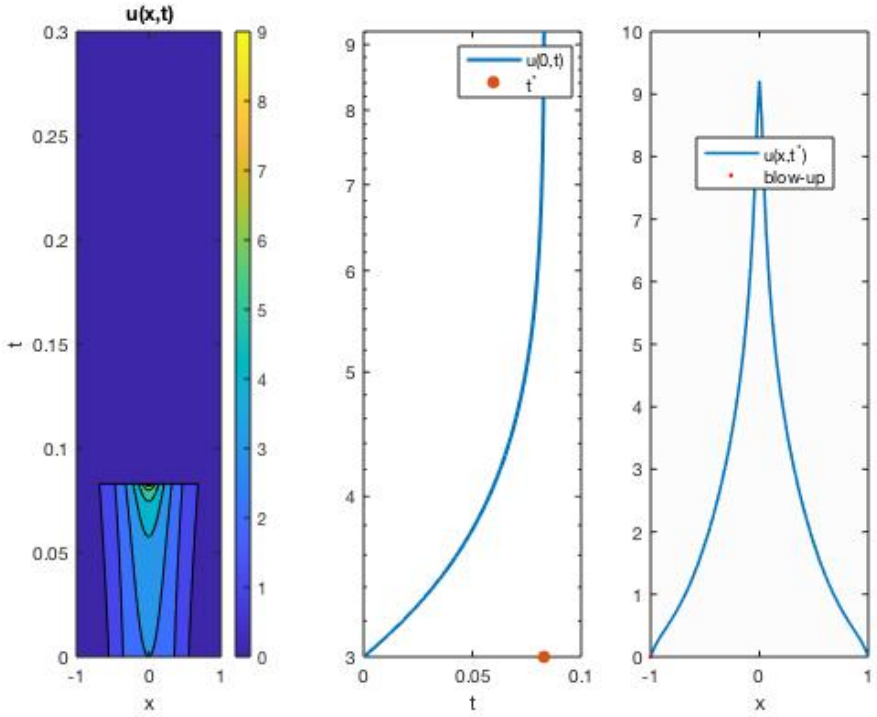

Figure 2.8: $\partial_t u + (-\Delta)^{\alpha/2} u = e^u, x \in (-1, 1)$, $\alpha = 1.5, H(s) = e^s - 1$, $T_\infty = 0.083040$.

Next, we compute the numerical blow-up time for different α-s. We can recognize a pattern similar to $f(u) = u^2$. We notice that the T_∞ and T_1 numerical blow-up times are different as it was expected, and the difference is within the following range $(0.00036, 0.00048)$.

Table 2.7: T_∞ and T_1 for $\partial_t u + (-\Delta)^{\alpha/2} u = e^u, x \in (-1,1), \gamma = 2, H(s) = e^s - 1$.

α	T_∞	T_1
0.5	0.057360	0.057720
0.8	0.060360	0.060720
1	0.063720	0.064080
1.3	0.072480	0.072960
1.5	0.083040	0.083520
1.7	0.099960	0.100320
1.9	0.125640	0.126000
1.999	0.141960	0.142440

We observe that the blow-up happens at a later time as α gets larger.

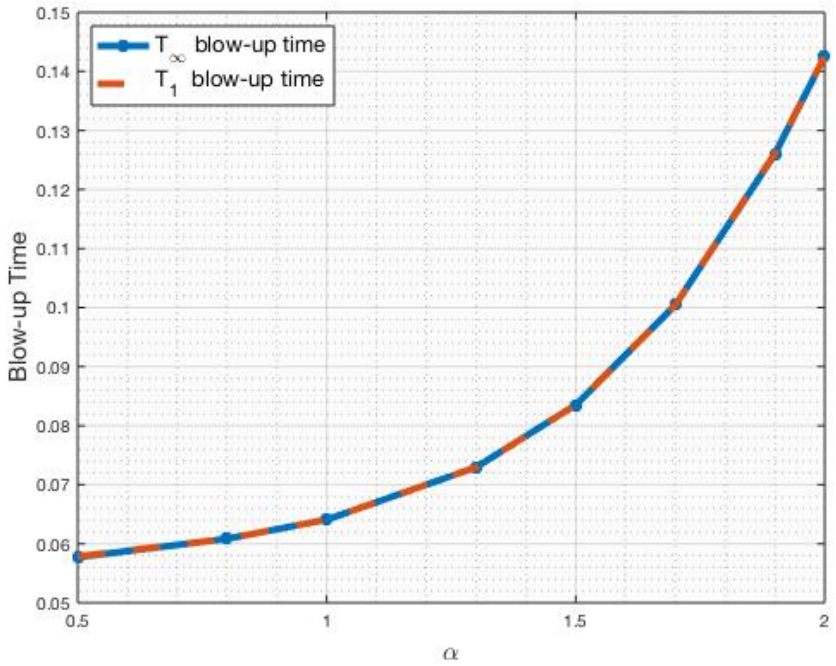

Figure 2.9: T_∞ and T_1 blow-up times using $\alpha \in [0.5, 1.999]$.

Next, we estimate blow-up times for different choices of α. We choose $H(s) = e^{2s} - 1$.

Table 2.8: T_∞ and T_1 for $\partial_t u + (-\Delta)^{\alpha/2} u = e^u, x \in (-1,1), \gamma = 2, H(s) = e^{2s} - 1$.

α	T_∞	T_1
0.5	0.045720	0.057600
0.8	0.048480	0.060600
1	0.051360	0.063960
1.3	0.059280	0.072120
1.5	0.068880	0.080760
1.7	0.084960	0.092760
1.9	0.110160	0.110400
1.999	0.126480	0.122520

We also estimate the blow-up times for different choices of the H function as there is no systematic way of choosing the optimal. We observe that for some cases the choice of the function H does not affect the blow-up time.

Table 2.9: T_∞ and T_1 for $\partial_t u + (-\Delta)^{\alpha/2} u = e^u, x \in (-1,1), \alpha = 1.5$.

$H(s) = e^{sm} - 1$	T_∞	T_1
m=0.5	0.083400	0.083520
m=1	0.083040	0.083520
m=1.1	0.082920	0.083400
m=1.3	0.081960	0.083400
m=4/3	0.081840	0.083400
m=3/2	0.080280	0.083400

Below is the illustration of blow-up when $\alpha = 1$ and $H(s) = e^{2s} - 1$. The estimated blow-up time is $T_\infty = 0.051360$.

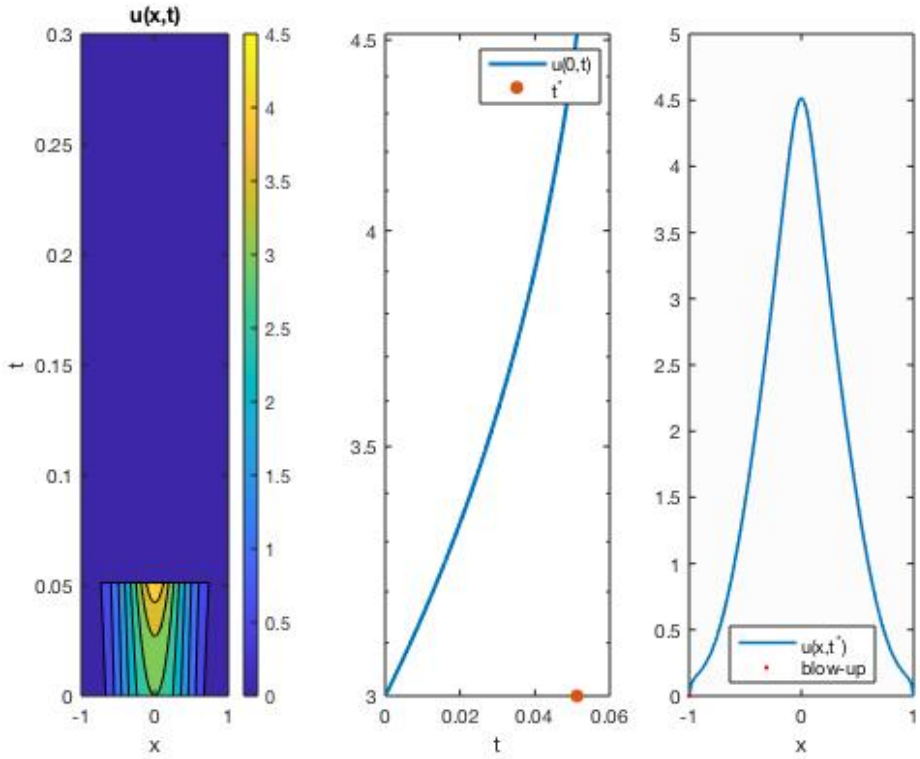

Figure 2.10: $\partial_t u + (-\Delta)^{\alpha/2} u = e^u, x \in (-1,1)$, $\alpha = 1, H(s) = e^{2s} - 1$, $T_\infty = 0.051360$.

2.3.3 Convergence Results

In this section, we would like to show mesh refinement. We fix the mesh ratio $\lambda = 0.3$ to ensure the stability and start to refine the time mesh by powers of 2 and compute the T_∞ and T_1 numerical blow-up times. Since $\lambda = 0.3$ and $\alpha = 1.5$ then by solving for h we get

$$h = \left(\frac{\tau}{0.3}\right)^{2/3}.$$

The tables below represent the estimated error and the rate for T_∞ and T_1 with $\alpha = 1.5$ and $H(s) = s$.

Table 2.10: T_∞, error and rate for $\partial_t u + (-\Delta)^{\alpha/2} u = u^2, x \in (-1,1), \gamma = 2$.

nt	time mesh τ	h	T_∞	error e	rate
2^4	0.01875000	0.15749013	0.093750	0.115306	1.16867269
2^5	0.00937500	0.09921257	0.065625	0.143431	0.84047137
2^6	0.00468750	0.06250000	0.056250	0.152806	0.67755673
2^7	0.00234375	0.03937253	0.100781	0.108275	0.68726313
2^8	0.00117188	0.02480314	0.214453	0.005397	1.41255499
2^9	0.00058594	0.01562500	0.212109	0.003053	1.39259278
2^{10}	0.00029297	0.00984313	0.210645	0.001589	1.39464977
2^{11}	0.00014648	0.00620079	0.210059	0.001003	1.35838127
2^{12}	0.00007324	0.00390625	0.209546	0.000490	1.37436633
2^{13}	0.00003662	0.00246078	0.209326	0.000270	1.36785611
2^{14}	0.00001831	0.00155020	0.209198	0.000142	1.36948087
2^{15}	0.00000916	0.00097656	0.209134	0.000078	1.36461664
2^{16}	0.00000458	0.00061520	0.209093	0.000037	1.38019830
2^{17}	0.00000229	0.00038755	0.209072	0.000016	1.40572664
2^{18}	0.00000114	0.00024414	0.209062	0.000006	1.44555051

Note that the error is defined defined as

$$e = |T_\infty - ref|$$

where ref is the reference blow-up time $T_\infty = 0.209056$ corresponding to $nt = 2^{19}$. The rate is

$$r = \frac{\log e}{\log h}$$

as

$$e = ch^r$$

where c is a constant.

We observe that a smaller time step results in a more refined blow-up time and a smaller error, i.e., from $nt = 2^4$ to $nt = 2^{18}$ we have an error refinement from 0.1153060 to 0.0000060 making a 0.1153000 difference. We can perform a similar analysis for the T_1 blow-up time.

Table 2.11: T_1, error and rate for $\partial_t u + (-\Delta)^{\alpha/2} u = u^2, x \in (-1, 1), \gamma = 2$.

nt	time mesh τ	h	T_1	error e	rate
2^4	0.01875000	0.15749013	0.037500	0.171558	0.95371188
2^5	0.00937500	0.09921257	0.075000	0.134058	0.86972123
2^6	0.00468750	0.06250000	0.056250	0.152808	0.67755200
2^7	0.00234375	0.03937253	0.103125	0.105933	0.69402343
2^8	0.00117188	0.02480314	0.216797	0.007739	1.31505696
2^9	0.00058594	0.01562500	0.213281	0.004223	1.31458601
2^{10}	0.00029297	0.00984313	0.211523	0.002465	1.29962950
2^{11}	0.00014648	0.00620079	0.210498	0.001440	1.28723393
2^{12}	0.00007324	0.00390625	0.209839	0.000781	1.29029873
2^{13}	0.00003662	0.00246078	0.209473	0.000415	1.29630012
2^{14}	0.00001831	0.00155020	0.209271	0.000213	1.30680632
2^{15}	0.00000916	0.00097656	0.209171	0.000113	1.31113896
2^{16}	0.00000458	0.00061520	0.209111	0.000053	1.33159201
2^{17}	0.00000229	0.00038755	0.209081	0.000023	1.35953000
2^{18}	0.00000114	0.00024414	0.209066	0.000008	1.41096405

Note that for this case the reference blow-up time is $T_1 = 0.209058$ corresponding to $nt = 2^{19}$. Hence, error refinement from 2^4 to 2^{18} is 0.171550.

The plot below represents the numerical blow-up times corresponding to different time steps, in particular to $nt = 2^8, 2^9, 2^{10}, 2^{11}$... and etc. We can see from the plot that estimated blow-up times converge to their reference blow-up times, $T_\infty = 0.209056$ and $T_1 = 0.209058$.

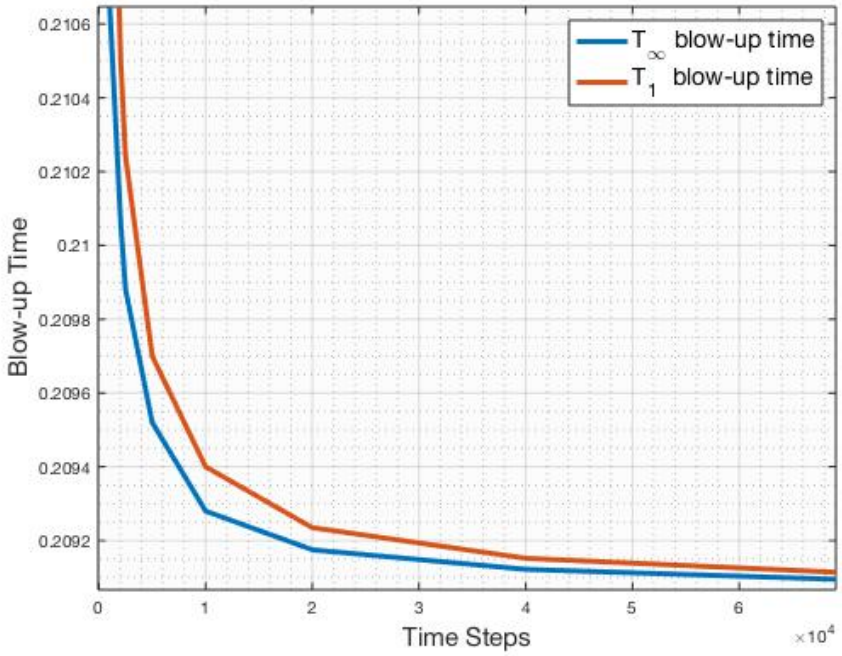

Figure 2.11: T_∞ and T_1 blow-up times convergence with respect to different time steps for a fixed λ. $\partial_t u + (-\Delta)^{\alpha/2} u = u^2, x \in (-1, 1)$, with $\alpha = 1.5, H(s) = s$.

We observe that the error approaches to 0 when the time mesh τ gets smaller. The plots below confirm that as long as the space mesh h ($\log(h)$) gets finer, the error ($\log(e)$) gets closer to zero.

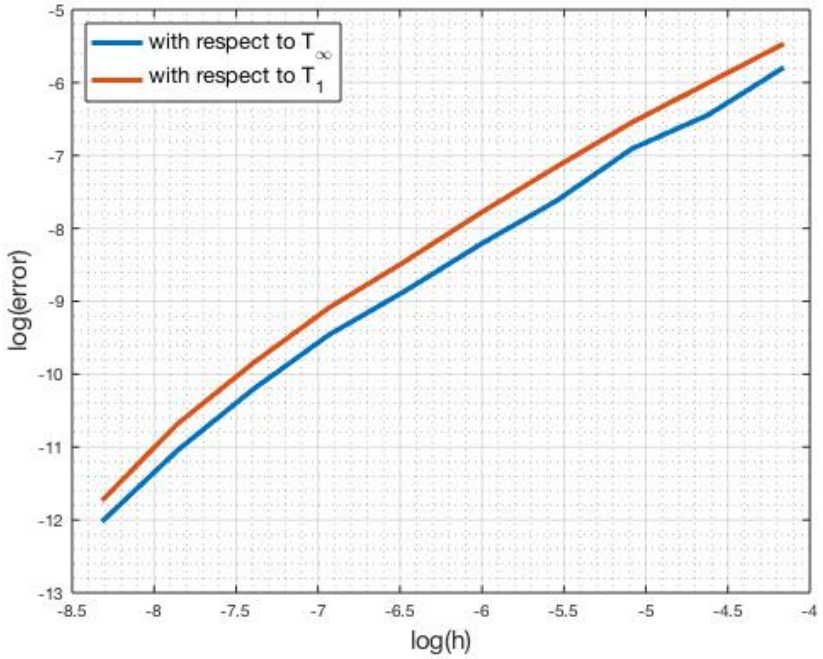

Figure 2.12: Mesh in space ($\log h$) with respect to errors ($\log e$) for T_∞ and T_1.

2.3.4 FPDE ($\alpha \to 2$) and PDE ($\alpha = 2$) Comparison

In this section, we would also like to make a comparison between a PDE and an FPDE when classical and fractional Laplace operators are considered, respectively. The goal is to inspect how close the computed blow-up times are when the central difference scheme is used for the PDE, i.e., $\alpha = 2$, and a weighted trapezoidal rule is used for the FPDE with $\alpha = 1.999$. In order to make the comparison the same choice of $H(s) = s$ is considered. The initial condition is

$$u(0,x) = u_0 = \begin{cases} 7(1-x^2)^{1+m} & x \in (-1,1) \\ 0 & else \end{cases}$$

and the Dirichlet boundary condition is

$$u(x,t) = 0 \quad x \in R \setminus \Omega, t > 0.$$

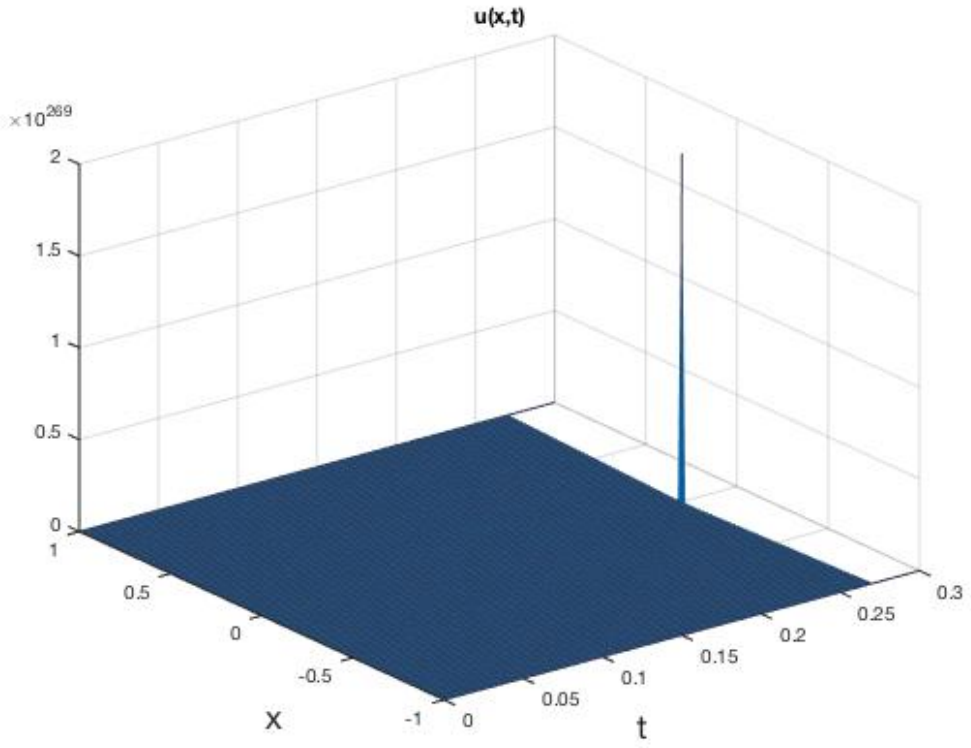

Figure 2.13: $u_t - u_{xx} = u^2, x \in \Omega = (-1,1), t > 0$ with $\tau = \dfrac{0.3}{50^2}$.

First, we consider Equation (1.2) with 0 boundary conditions and with the following reaction term $f(u) = u^2$. Spatial grid size is chosen such that $\lambda = \dfrac{\tau}{h^2} = 0.3$ is less than 0.5. The numerical blow-up time for the classical heat equation with an appropriate boundary and large enough initial condition is $T_\infty = 0.264000$. See Figure 2.13.

Next, consider the fractional problem again with 0 boundary conditions, illustrated in Figure 2.14. Note that the $\lambda = 0.2988$ in this case. The numerical blow-up time for the fractional PDE is $T_\infty = 0.263760$.

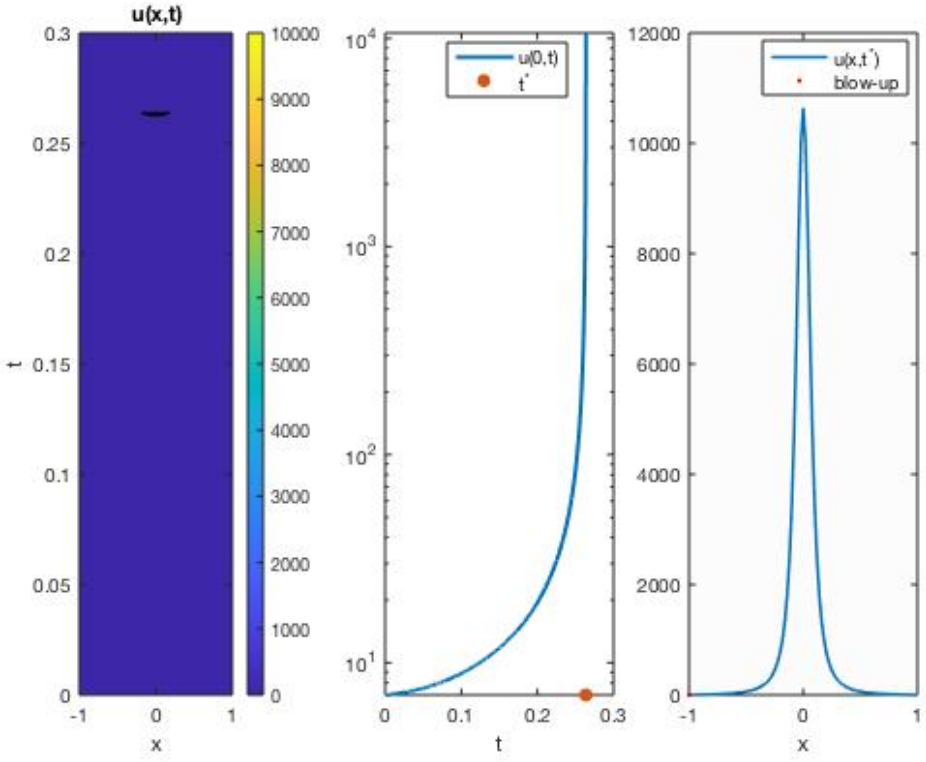

Figure 2.14: $\partial_t u + (-\Delta)^{\alpha/2} u = u^2, x \in (-1, 1)$, $\alpha = 1.999$, $\gamma = 2$, $T_\infty = 0.263760$.

We observe that numerical blow-up times detected by numerical algorithms for the classical and fractional reaction-diffusion equation are different by an amount of 0.00024 when the same boundary and initial conditions are considered. Hence, we can claim that the numerical algorithm implemented to discretize the fractional reaction-diffusion equation provides an accurate blow-up time.

2.4 Conclusions

We studied the blow-up phenomena and estimated blow-up times for an important evolution equation, in particular for the fractional reaction-diffusion equation with appropriate initial and boundary conditions. We adapted the already existing novel and accurate discretization method of the fractional Laplacian with an auxiliary function H such that the discretization will detect blow-up time. We numerically estimated blow-up time for the fractional reaction-diffusion equation with two different reaction terms, particularly $f(u) = u^2$ and $f(u) = e^u$. We computed blow-up times for different choices of α and H. We showed that T_1 and T_∞ blow-up times are different as expected, and the difference is in a particular range. For the exponential reaction term, we observe that several choices of function H did not affect the blow-up time. We proved several important convergence and error estimate results. We made a comparison of an FPDE when $\alpha \to 2$, and a PDE when $\alpha = 2$ and got consistent results. The detected blow-up times for the FPDE and PDE are $T_\infty = 0.263760$ and $T_\infty = 0.264000$, respectively. In addition, stability conditions were satisfied.

Chapter 3

Blow-ups with Adaptive Moving Mesh Methods

Moving mesh methods are commonly used in numerical analysis. They can help to achieve higher accuracy. For example, one might consider adding more elements in the regions with rapid changes, or in the systems with possible blow-up solutions. For such problems use of a uniform mesh can be a major computational expense. Hence, sometimes an essential alternative is to place a large proportion of mesh points in regions of wide variation of solution and only a few points in the rest of the domain. This is the idea of mesh adaptivity.

3.1 Introduction

We start this with an important discussion. How should mesh points be chosen? We start with choosing mesh density function $\rho(x)$. So, where the $\rho(x)$ is larger, the distances between mesh points are smaller and the other way around. The square of the mesh density function is called monitor function. However, in some literature the ρ is typically referred to as monitor function [13, 15, 34, 32, 31, 52]. Let's define monitor function as

$$M = \rho^2(x)$$

The distance between two points in 1D is given by

$$\int_a^b \sqrt{det(M)}dx = \int_a^b \rho(x)dx.$$

Another, sightly different method is to consider the approximation of the function. In this case the monitor function is given by

$$\rho = \sqrt{1 + \frac{1}{\alpha}\left(\frac{du}{dx}\right)^2}.$$

The discussion of this section is based on [33].

A blow-up solution often represents a significant change in the characteristics of the model. It can be associated with explosion or self-ignition. Hence, it is of great practical interest to have an accurate numerical approximation. One way to deal with this problem is to consider adaptive time mesh methods.

Consider the following reaction-diffusion classical model which has been extensively studied in the past

$$\begin{aligned} u_t &= u_{xx} + u^p \\ u(0,t) &= u(1,t) = 0 \\ u(x,0) &= u_0(x) > 0 \end{aligned} \tag{3.1}$$

where $u_0(x)$ is a given initial solution. It is known that if the initial solution is large enough the solution blows-up in finite time

$$x* \in (0,1) \quad \text{as} \quad t \to T. \tag{3.2}$$

x^* and T are known as blow-up space and time. The blow-up profile of the solution is more precisely studied and described in [33, 7]. It can be best shown if we look at the kernel coordinate

$$\mu = (x - x*)[(T-t)(\alpha - \log(T-t))]^{-1/2}.$$

An MMPDE (moving mesh partial differential equation), in particular MMPDE5 will be used here. A coordinate transformation

$$x(\xi,t) = x^* + (T-t)^{1/2}[\alpha - \log(T-t)]^{1/2} z(\xi,t)$$

with the following property

$$z(\xi, t) = z_0(\xi) + o(1)$$

is generated.

An MMDPE5 is applied to discretize the classical reaction-diffusion equation. As $t \to T$

$$\|u\|_\infty \approx (T-t)^{-\beta}\beta^\beta$$

and

$$\frac{u}{\|u\|_\infty} \to \left(1 - 4(\xi - \frac{1}{2})^2\right)^\beta.$$

$$\begin{aligned}\log|x - x^*| \to -\frac{1}{2\beta}\log\|u\|_\infty + \log\frac{4\sqrt{p\beta}(\xi_i - 1/2)}{\sqrt{1-4(\xi_i-1/2)^2}} \\ + \frac{1}{2}\beta + \frac{1}{2}\log\left[\alpha + \frac{1}{\beta}\log\|u\|_\infty - \log\beta\right] \\ - \frac{1}{2\beta}\log\|u\|_\infty + c_i \quad (3.3)\end{aligned}$$

where c_i is a constant depending on ξ_i.

3.2 Preliminary Results

In this section we work with PDEs and use adaptive moving mesh methods to estimate the blow-up times numerically.

3.2.1 Reaction-Diffusion Equation with Moving Mesh Methods

We start with the following PDE

$$\begin{aligned}u_t &= u_{xx} + u^2 \\ u(0,t) &= u(1,t) = 0 \\ u(x,0) &= 100\sin(\pi x)\end{aligned} \quad (3.4)$$

where $0 < x < 1$ and $t > 0$. Applying coordinate transformation on (3.4) based on [32] we get

$$\frac{\partial u}{\partial t} - \frac{\partial u}{\partial x}\frac{\partial x}{\partial t} = \frac{\partial^2 u}{\partial x^2} + u^2.$$

The idea is to write the PDE with derivatives taken only with respect to t

$$\frac{du}{dt} - \Delta u \frac{dx}{dt} = \Delta^2 u + u^2 := g(u).$$

MMPDE6 and the following monitor function (or mesh density) is considered

$$\rho(x,t) = \sqrt{1 + \left(\frac{du_i}{dx_i}\right)^2}.$$

We then get the following system

$$\begin{aligned}
\frac{du_1}{dt} - \Delta u_1 \frac{dx_1}{dt} &= \Delta^2 u_1 + u_1^2 \\
&\vdots \\
\frac{du_N}{dt} - \Delta u_N \frac{dx_N}{dt} &= \Delta^2 u_N + u_N^2 \\
\frac{d^2\dot{x_1}}{dt^2} &= \frac{1}{\tau}\frac{d}{dt}\left(\rho(x_1,t)\frac{dx_1}{dt}\right) \\
&\vdots \\
\frac{d^2\dot{x_N}}{dt^2} &= \frac{1}{\tau}\frac{d}{dt}\left(\rho(x_N,t)\frac{dx_N}{dt}\right).
\end{aligned} \tag{3.5}$$

The left-hand side of the system (3.5) can be summarised as

$$\begin{bmatrix} M_1 & M_2 \\ M_3 & M_4 \end{bmatrix} \begin{bmatrix} \dot{u_1} \\ \vdots \\ \dot{u_N} \\ \dot{x_1} \\ \vdots \\ \dot{x_N} \end{bmatrix}$$

where

$$M_1 = I_N$$
$$M_2 = -\frac{\partial u_i}{\partial x_i} I_N$$
$$M_3 = 0_N$$
$$M_4 = \frac{\partial^2}{\partial t^2} I_N.$$

The discretized g_i with centered finite differences is given

$$g_i = \frac{\dfrac{u_{i+1} - u_i}{x_{i+1} - x_i} - \dfrac{u_i - u_{i-1}}{x_i - x_{i-1}}}{0.5(x_{i+1} - x_{i-1})} + u_i^2. \tag{3.6}$$

To approximate the monitor function ρ finite differences is used as follows

$$\rho(x,t) = \sqrt{1 + \left(\frac{u_{i+1} - u_{i-1}}{x_{i+1} - x_{i-1}}\right)^2}.$$

3.2.2 Numerical Experiments

Theoretically it is know that we should expect a blow-up for Problem 3.4. Moreover, from Cho [18] we know that T_1 or the T_∞ blow-up times are 0.0109883 and 0.0109875, respectively.

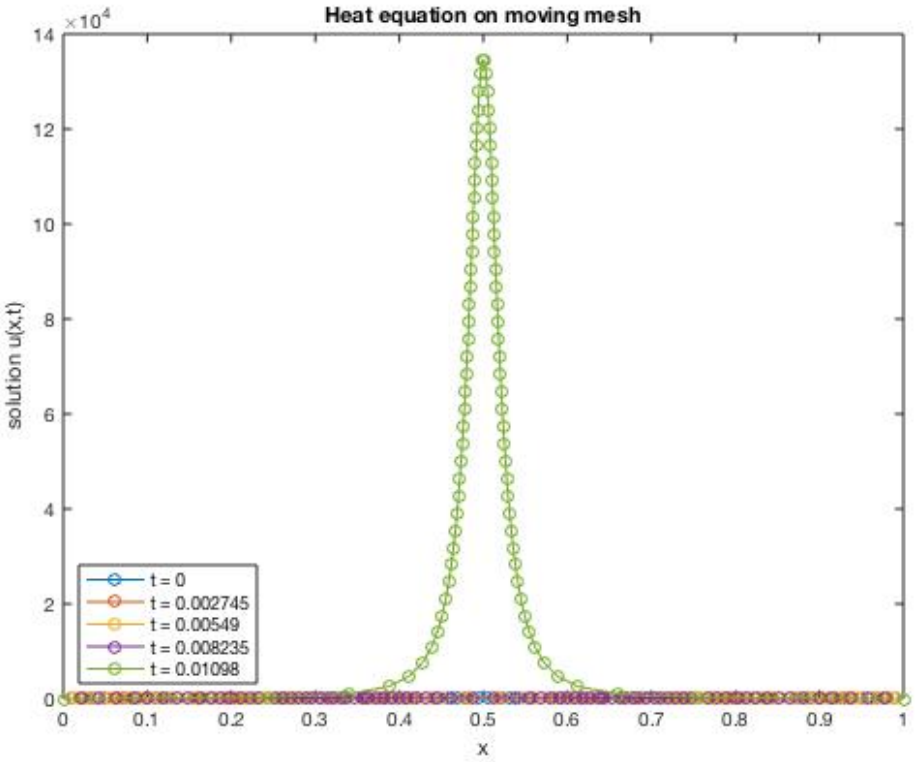

Figure 3.1: $u_t = u_{xx} + u^2$ with $u(x, 0) = 100 \sin(\pi x)$, $0 < x < 1$ and $t > 0$.

Figure 3.2 is a plot of trajectories of grid points. Due to the monitor function the mesh points are clustered at discontinuity(blow-up).

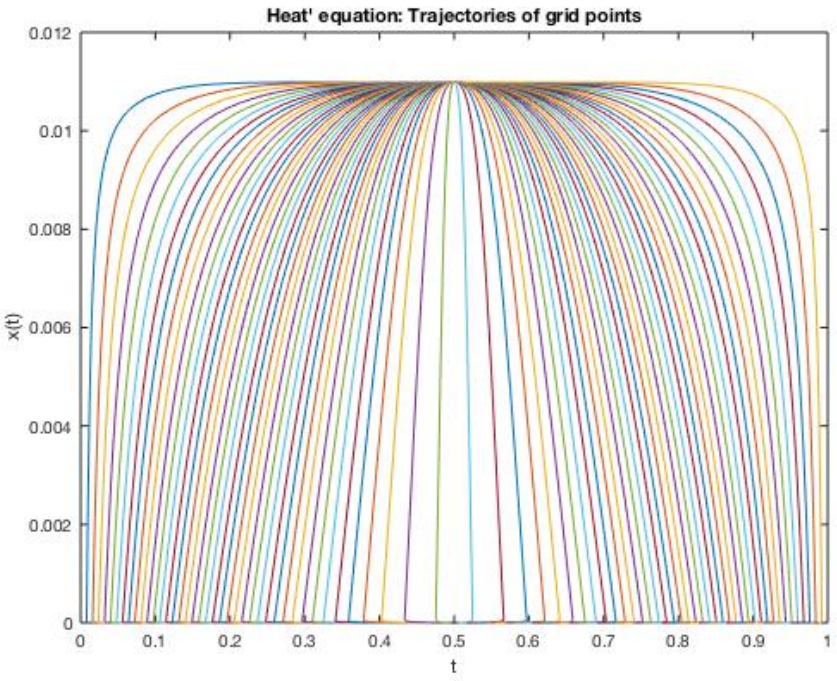

Figure 3.2: The movement of the mesh points.

We observe the change in the solution $u(x,t)$ when the time t experiences small changes.

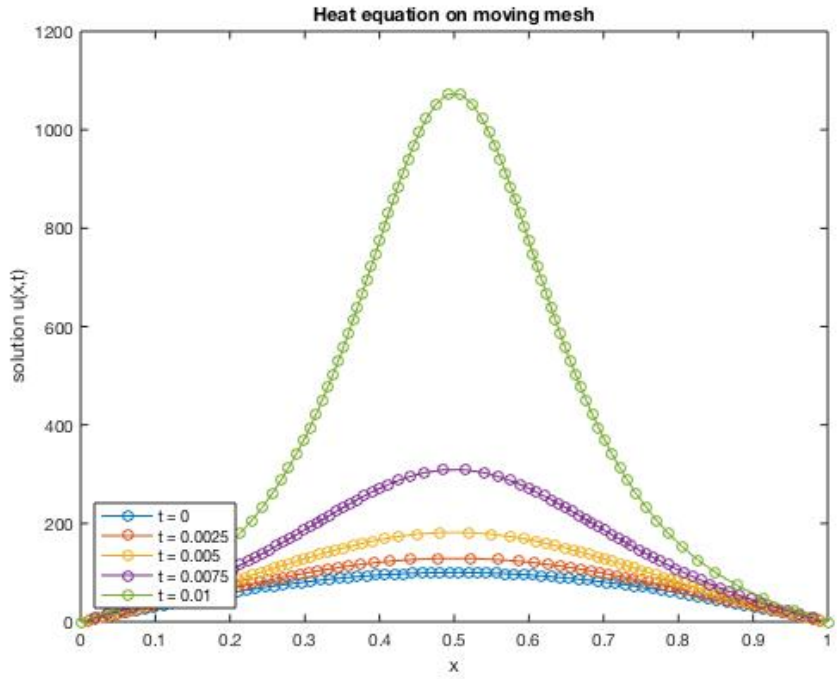

Figure 3.3: $u_t = u_{xx} + u^2$ with $u(x,0) = 100\sin(\pi x)$, $0 < x < 1$ and $t > 0$.

Next, we overlay the solutions for different choices of t, already knowing that the T_∞ blow-up happens at 0.010987 according to [18]. We observe that the solution gets larger as the time approaches the blow-up time.

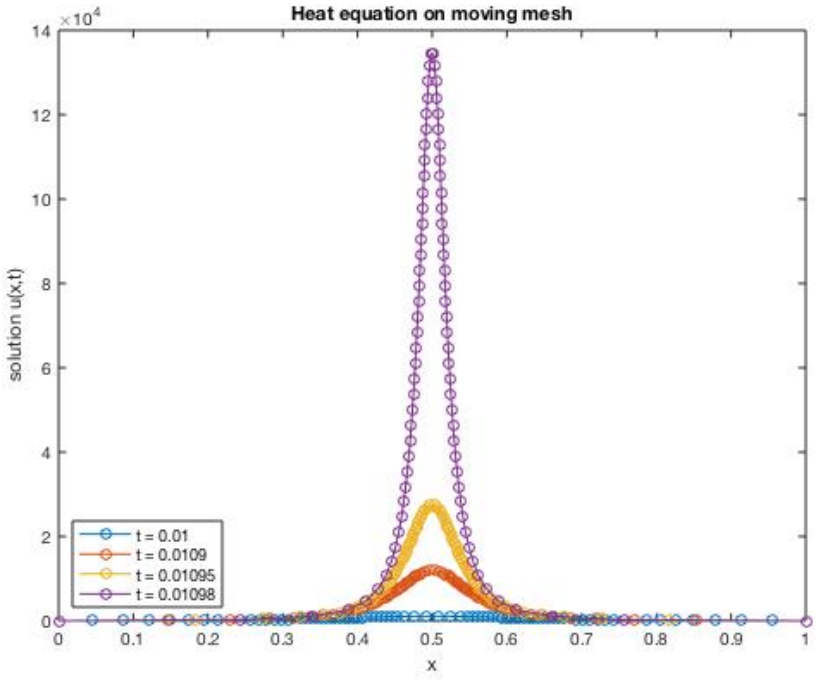

Figure 3.4: $u_t = u_{xx} + u^2$ with $u(x,0) = 100\sin(\pi x)$, $0 < x < 1$ and $t > 0$.

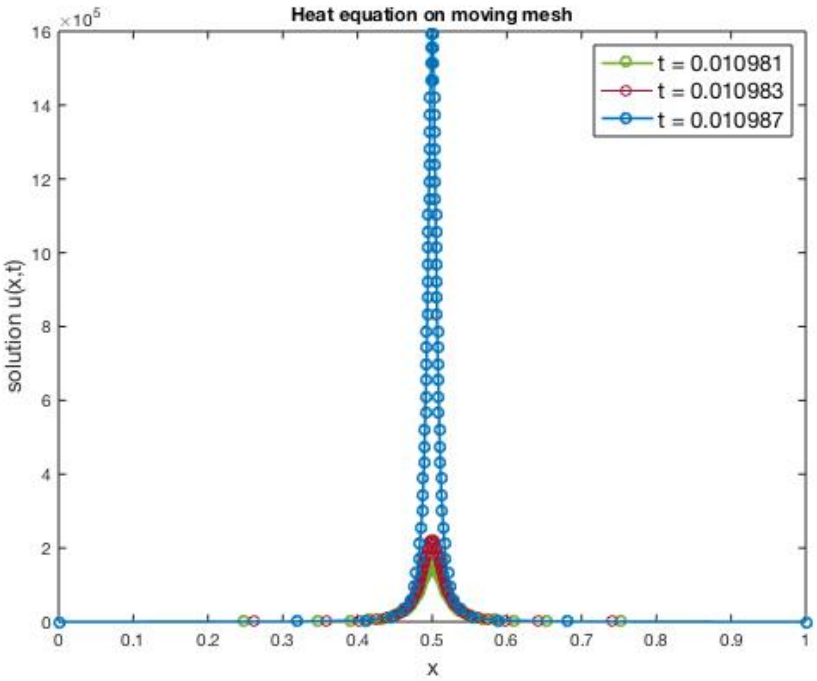

Figure 3.5: $u_t = u_{xx} + u^2$ with $u(x,0) = 100\sin(\pi x)$, $0 < x < 1$ and $t > 0$.

In Figure 3.5, we have a better approximation of the blow-up time. We plot the solution to the Equation (3.4) for $t = 0.010981, 0.010983, 0.010987$.

Now, we consider Equation (3.4) but with a different initial condition

$$\begin{aligned} u_t &= u_{xx} + u^2 \\ u(0,t) &= u(1,t) = 0 \\ u(x,0) &= 20\sin(\pi x) \end{aligned} \tag{3.7}$$

We want to discretize the problem such that we will detect the blow-up time numerically. We apply the discretization scheme described in Section 3.2.1. As we would expect, there is a peak around $x^* = 0.5$ which is the center of the interval. The numerical blow-up time is detected, and it is estimated to be $T^* = 0.082466$. This confirms the result obtained in [46]. However, a different choice of monitor function was considered in the work of R. Marlow. Hence, our blow-up time is different from the blow-up time obtained in [46].

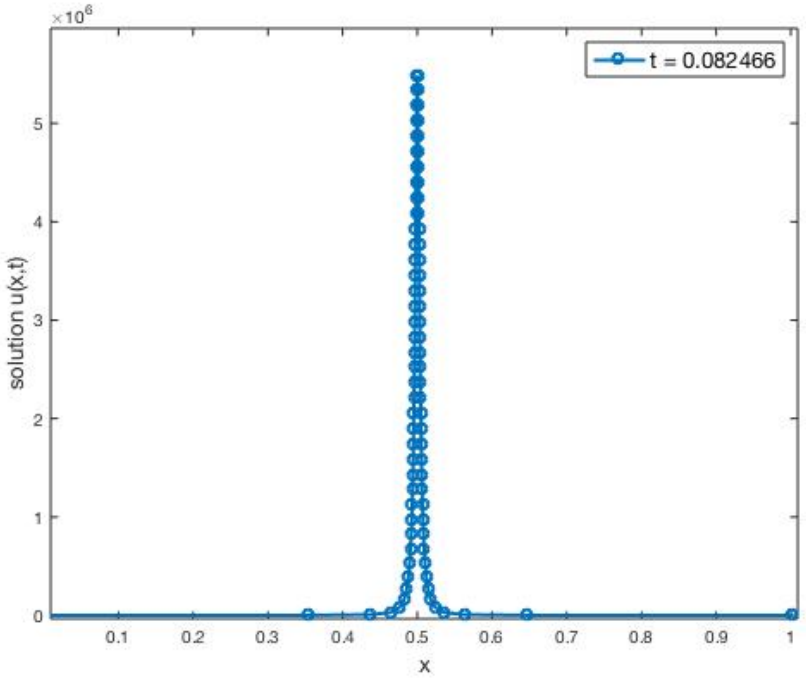

Figure 3.6: $u_t = u_{xx} + u^2$ with $u(x,0) = 20\sin(\pi x)$, $0 < x < 1$ and $t > 0$.

It is theoretically known that we should also expect a blow-up for the case when the reaction term is $f(u) = u^3$. The estimated blow-up time is $T^* = 0.0012816$. We notice that the solution reached its peak.

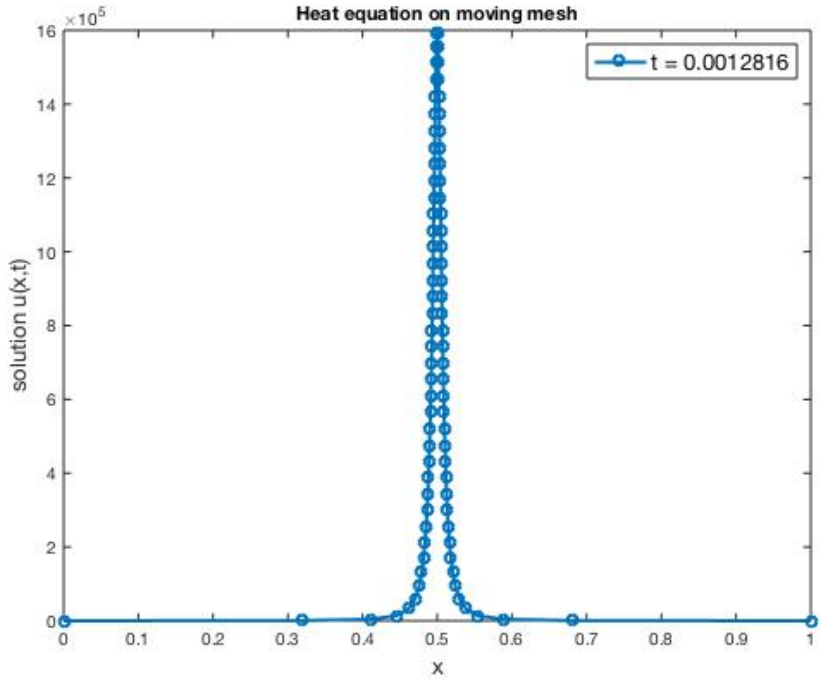

Figure 3.7: $u_t = u_{xx} + u^3$ with $u(x, 0) = 100 \sin(\pi x)$, $0 < x < 1$ and $t > 0$.

We also estimate the numerical blow-up time for

$$\begin{aligned} u_t &= u_{xx} + e^u \\ u(0, t) &= u(1, t) = 0 \\ u(x, 0) &= 5 \sin(\pi x). \end{aligned} \tag{3.8}$$

Using ODE solver ode15s we estimate the numerical blow-up time to be $T^* = 0.0098486$. We also use another ODE solver, ode23t, which is more efficient to solve problems that are error sensitive. We estimate the blow-up time to be $T^* = 0.0098449$.

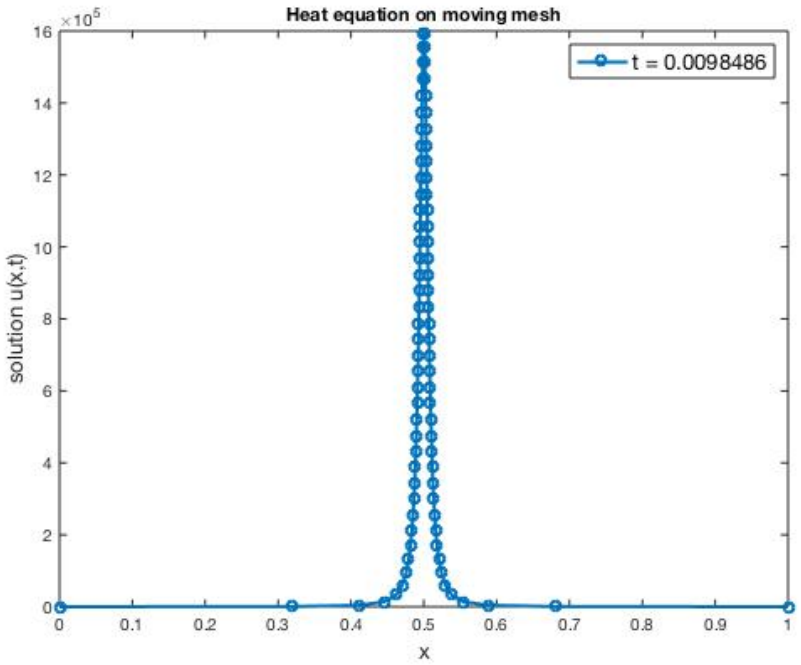

Figure 3.8: $u_t = u_{xx} + e^u$ with u $(x, 0) = 5\sin(\pi x)$, $0 < x < 1$ and $t > 0$.

Next, we choose the initial condition to be $u(x, 0) = 20\sin(\pi x)$ then the blow-up results will be comparable to the case when $f(u) = u^2$. The estimated blow-up time is $T^* = 2.0652e^{-09}$. As we would expect, the blow-up for the exponential case occurs earlier compared to u^2 given the same initial conditions.

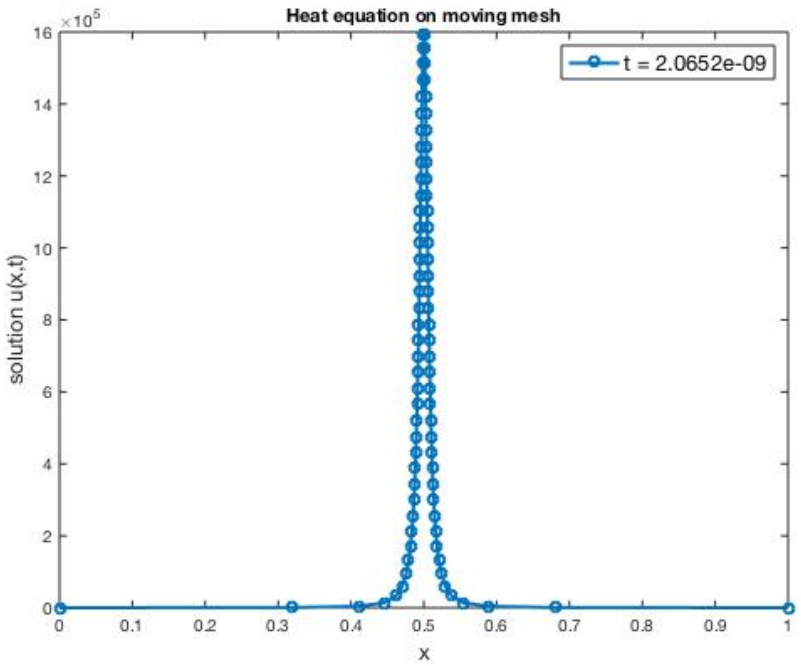

Figure 3.9: $u_t = u_{xx} + e^u$ with u $(x, 0) = 20\sin(\pi x)$, $0 < x < 1$ and $t > 0$.

3.3 Conclusions

In this chapter, we used adaptive moving mesh techniques [32] to numerically estimate the blow-up times of reaction-diffusion equations. We notice that due to the monitor function the mesh points are clustered at the discontinuity(blow-up). For the reaction-diffusion equation with $f(u) = u^2$ and $u_0 = 100\sin(\pi x)$, $u_0 = 20\sin(\pi x)$ the estimated numerical blow-up times are $T^* = 0.010987$ and $T^* = 0.082466$, respectively. For $f(u) = u^3$ with $u_0 = 20\sin(\pi x)$ the blow-up time $T^* = 0.0012816$. We compared the blow-up times of $f(u) = e^u$ with $f(u) = u^2$ for a fixed initial condition $u_0 = 20\sin(\pi x)$. The estimated blow-up time for the exponential case is $T^* = 2.0652e^{-09}$. We observe that the blow-up happens earlier compared to u^2 which was expected.

Chapter 4

Future Work

4.1 Fractional Reaction-Diffusion Equation Blow-ups with Adaptive Meshes

The blow-up phenomena [3, 54, 12, 57, 35] of space-time reaction-diffusion equations [14, 56, 4, 37, 38] have been intensively studied in previous years. However, the numerical estimation of blow-up time remains partially understood. Most numerical methods developed so far include fixed-mesh methods. However, as far as the blow-up phenomenon is concerned, the moving mesh methods have been considered effective since the invention by Budd et al. [11]. JingTang and YingJun in [45] proposed a moving collocation method to solve time-fractional differential equations, in particular for

$$\frac{\partial u}{\partial t} = D_t^{1-\alpha}\Big[\frac{\partial^2 u}{\partial x^2}\Big] + f(x,t,u), \quad -1 \le x \le 1, 0 < t \le T$$

with initial and boundary conditions

$$u(x,0) = u_0(x),$$
$$u(-1,t) = u_L(t), u(1,t) = u_R(t),$$

where $D_t^{1-\alpha}, 0 < \alpha \le 1$ is a Riemann-Liouville derivative defined as

$$D_t^{1-\alpha}u(x,t) = \frac{1}{\Gamma(\alpha)}\frac{\partial}{\partial t}\int_0^t (t-\tau)^{\alpha-1}u(x,\tau)d\tau.$$

They used the proposed method to simulate the blow-up and estimated the blow-up time numerically. Again, the need for discretizing the differential equations, in particular fractional differential equations, is that they have no analytical forms of solution. Hence,

the next FPDE we propose to solve with adaptive moving mesh methods in the future is

$$\partial_t u + (-\Delta)^{\alpha/2} u = f(u).$$

We aim to estimate blow-up times numerically and compare them with results we obtained in Section 2.3.

We studied the following time fractional reaction-diffusion equation

$$\begin{aligned} {}^{C}D^{\beta}u - u_{xx} &= u^p, x \in \Omega, t > 0 \\ u(x,t) &= 0, x \in \partial\Omega, t > 0 \\ u(x,0) &= u_0(x), x \in \Omega \end{aligned} \tag{4.1}$$

where ${}^{C}D^{\beta}u(t)$, the Caputo derivative of fractional order $\beta > 0$, is defined as

$${}^{C}D^{\beta}u(t) = \frac{1}{\Gamma(n-\beta)} \int_0^t (t-\tau)^{n-\beta-1} u^{(n)}(\tau) d\tau.$$

where $n - 1 < \beta < n$. Kirane et al. in [39] obtained the critical exponents for the space-time fractional equation, which are the generalizations of the results by Fujita [26] known as the Fujita exponent. Pursuing the numerical estimation of blow-up times for Equation (4.1) we studied and applied piecewise constant approximation from [5] to discretize the Caputo fractional derivative ${}^{C}D^{\beta}u(t)$. The idea is to neglect the u_{xx} term and consider the more general reaction term $G(u)$. Hence, Equation (4.1) simplifies to the following fractional differential equation (FDE)

$$\begin{aligned} {}^{C}D^{\beta}u(t) &= G(u) \\ u(0) &= u_0. \end{aligned} \tag{4.2}$$

The discretized solution is

$$u(n\Delta t) = u_0 + \frac{(n\Delta t)^\beta}{\Gamma(1+\beta)} G(u_0) + \sum_{m=1}^{n-1} \frac{((n-m)\Delta t)^\beta}{\Gamma(1+\beta)} \big(G(u(m\Delta t)) - G(u((m-1)\Delta t))\big).$$

We can easily check that for $\beta = 1$ the discretization simplifies to the Euler method. If we take $\beta = 1$ and $G(u) = u^2$ in (4.2) then we know the solution is explicitly given by

$$u(t) = \frac{u_0}{1 - u_0 t}.$$

When $u_0 = 1$ the solution to this ODE should blow up at $T = 1$. We observe this also by plotting it. Moreover, we plot the numerical solution with piecewise constant approximation scheme. However, the scheme does not detect the blow-up at 1. Hence, one should implement a suitable scheme that will detect the blow-up time.

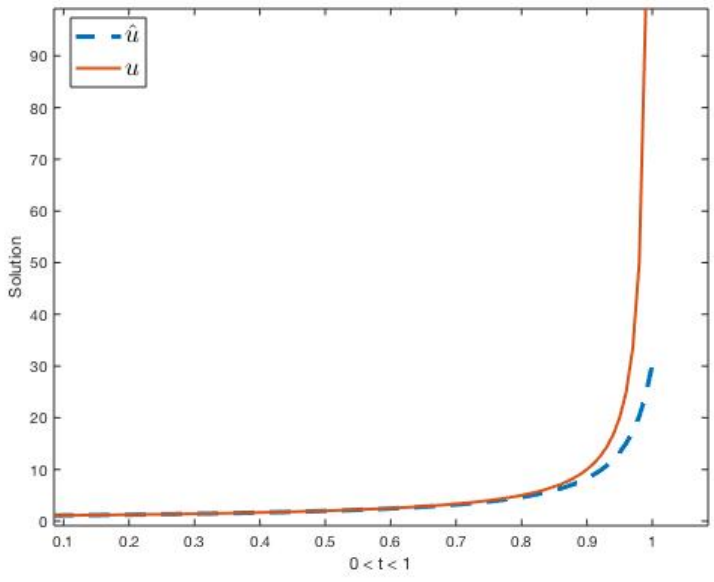

Figure 4.1: Exact and numerical solutions to $u'(t) = u^2$.

Bibliography

[1] L.M. Abia, J.C. López-Marcos, and J. Martinez. The euler method in the numerical integration of reaction–diffusion problems with blow-up. *Applied Numerical Mathematics*, 38(3):287–313, Aug 2001.

[2] Lidia Aceto and Paolo Novati. Rational approximation to the fractional laplacian operator in reaction-diffusion problems. *SIAM Journal on Scientific Computing*, 39, 07 2016.

[3] Ahmed Alsaedi, Mokhtar Kirane, and Berikbol Torebek. Global existence and blow-up for a space and time nonlocal reaction-diffusion equation. *Quaestiones Mathematicae*, 44:1–7, 07 2020.

[4] Edgardo Alvarez, Ciprian G. Gal, Valentin Keyantuo, and Mahamadi Warma. Well-posedness results for a class of semi-linear super-diffusive equations. *Nonlinear Analysis, Theory, Methods and Applications*, 181, 08 2018.

[5] Christopher Angstmann, B. Henry, Byron Jacobs, and Anna McGann. Discretization of fractional differential equations by a piecewise constant approximation. *Mathematical Modelling of Natural Phenomena*, 12, 12 2017.

[6] Vo Anh, Milos Ilic, F. Liu, and Ian Turner. Numerical approximation of a fractional-in-space diffusion equation (ii) - with nonhomogeneous boundary conditions. *Fractional Calculus and Applied Analysis*, 9, 01 2006.

[7] J. Bebernes and S. Bricher. Final time blowup profiles for semilinear parabolic equations via center manifold theory. *Siam Journal on Mathematical Analysis - SIAM J MATH ANAL*, 23, 07 1992.

[8] Becherer and Martin Schweizer. Classical solutions to reaction-diffusion systems for hedging with interacting itô and point processes. *Annals of Applied Probability*, pages 1111–1144, 2005.

[9] Dirk Becherer. Utility indifference hedging and valuation via reaction diffusion systems. *Proceedings of The Royal Society A: Mathematical, Physical and Engineering Sciences*, 460:27–51, 01 2004.

[10] Piotr Biler, Grzegorz Karch, and Wojbor A Woyczyński. Critical nonlinearity exponent and self-similar asymptotics for levy conservation laws. *Annales de l'I.H.P. Analyse non lineaire*, 18(5):613–637, 2001.

[11] C. Budd, Weizhang Huang, and Robert Russell. Moving mesh methods for problems with blow-up. *SIAM Journal on Scientific Computing*, 17:305–327, 02 1996.

[12] Jianxiong Cao, Guojie Song, Jie Wang, Qihong Shi, and Sujing Sun. Blow-up and global solutions for a class of time fractional nonlinear reaction–diffusion equation with weakly spatial source. *Applied Mathematics Letters*, 91, 12 2018.

[13] Weiming Cao, Weizhang Huang, and D. Russell. A study of monitor functions for two-dimensional adaptive mesh generation. *SIAM Journal on Scientific Computing*, 20:1978–1994, 12 1999.

[14] Alexandre Carvalho, Paulo Carvalho, Pedro Marín-Rubio, and Bruno de Andrade. Semilinear fractional differential equations: Global solutions, critical nonlinearities and comparison results. *Topological Methods in Nonlinear Analysis*, 45:439, 06 2015.

[15] Héctor D. Ceniceros and Thomas Y. Hou. An efficient dynamically adaptive mesh for potentially singular solutions. *Journal of Computational Physics*, 172:609–639, 2001.

[16] Yungang Chen. Asymptotic behaviours of blowing-up solutions for finite difference analogue of $u_t = u_{xx} + u^{1+\alpha}$. *J. Fac. Sci., Univ. Tokyo, Sect. I A*, 33:541–574, 1986.

[17] C. Cho, S. Hamada, and H. Okamoto. On the finite difference approximation for a parabolic blow-up problem. *Japan Journal of Industrial and Applied Mathematics*, 24:131–160, 2007.

[18] Chien-Hong Cho. On the computation of the numerical blow-up time. *Japan Journal of Industrial and Applied Mathematics*, 30(2):331–349, jan 2013.

[19] Heyrim Cho and D. Levy. Modeling the chemotherapy-induced selection of drug-resistant traits during tumor growth. *Journal of Theoretical Biology*, 436, 10 2017.

[20] Jerome Coville, Changfeng Gui, and Mingfeng Zhao. Propagation acceleration in reaction diffusion equations with anomalous diffusions. *Nonlinearity*, 34:1544–1576, 03 2021.

[21] Félix del Teso, David Gómez-Castro, and Juan Luis Vazquez. Three representations of the fractional p-laplacian: semigroup, extension and balakrishnan formulas. 10 2020.

[22] Keng Deng and Howard Levine. The role of critical exponents in blow-up theorems: The sequel. *Journal of Mathematical Analysis and Applications*, 243:85–126, 03 2000.

[23] Siwei Duo, Hans Wyk, and Yanzhi Zhang. A novel and accurate finite difference method for the fractional laplacian and the fractional poisson problem. *Journal of Computational Physics*, 355, 11 2017.

[24] Muhamed Farouq, Wadii Boulila, Zain Hussain, Asrar Rashid, Moiz Shah, Sajid Hussain, Nathan Ng, Dominic Ng, Haris Hanif, Mohamad Shaikh, Aziz Sheikh, and Amir Hussain. A novel coupled reaction-diffusion system for explainable gene expression profiling. *Sensors*, 21:2190, 03 2021.

[25] Ahmad Fino and Grzegorz Karch. Decay of mass for nonlinear equation with fractional Laplacian. June 2008. 9 pages.

[26] H. Fujita. On the blowing up of solutions of the cauchy problem for $u_t = \delta u + u^{1+\alpha}$. 1966.

[27] M. Guedda and Mokhtar Kirane. A note on nonexistence of global solutions to a nonlinear integral equation. *Bulletin of the Belgian Mathematical Society - Simon Stevin*, 6, 10 1999.

[28] M. Guedda and Mokhtar Kirane. Criticality for some evolution equations. *Differential Equations*, 37:540–550, 04 2001.

[29] Y. Han, Xian Zhang, L. Wu, and Y. Wang. State estimation for genetic regulatory networks with time-varying delays and reaction-diffusion terms. *IEEE Transactions on Neural Networks and Learning Systems*, PP, 09 2015.

[30] K. Hayakawa. On nonexistence of global solutions of some semilinear parabolic differential equations. 1973.

[31] Ronald Haynes, Weizhang Huang, and Robert Russell. *A Moving Mesh Method for Time-dependent Problems Based on Schwarz Waveform Relaxation*, volume 60, pages 229–236. 12 2007.

[32] Weizhang Huang, Yuhe Ren, and Robert Russell. Moving mesh partial differential equations (mmpdes) based on the equidistribution principle. *SIAM Journal on Numerical Analysis*, 31:709–730, 06 1994.

[33] Weizhang Huang and Robert Russell. *Adaptive Moving Mesh Methods*, volume 174. 01 2011.

[34] Weizhang Huang and Weiwei Sun. Variational mesh adaptation ii: error estimates and monitor functions, 2003.

[35] Razvan Iagar and Ariel Sanchez. Blow up profiles for a reaction–diffusion equation with critical weighted reaction. *Nonlinear Analysis*, 191:111628, 02 2020.

[36] Milos Ilic, F. Liu, Ian Turner, and V Anh. Numerical approximation of a fractional-in-space diffusion equation, i. *Fractional Calculus and Applied Analysis (FCAA)*, 8, 01 2005.

[37] Jukka Kemppainen, Rico Zacher, and Juhana Siljander. Representation of solutions and large-time behavior for fully nonlocal diffusion equations. *Journal of Differential Equations*, 263, 03 2017.

[38] Valentin Keyantuo, Carlos Lizama, and Mahamadi Warma. Existence, regularity and representation of solutions of time fractional diffusion equations. *Advances in Differential Equations*, 21:837–886, 09 2016.

[39] M. Kiranea, Y. Laskrib, and N. e. Tatarc. Critical exponents of fujita type for certain evolution equations and systems with spatio-temporal fractional derivatives. 2005.

[40] Kusuo Kobayashi, T. Sirao, and H. Tanaka. On the growing up problem for semilinear heat equations. *Journal of The Mathematical Society of Japan*, 29:407–424, 1977.

[41] Christina Kuttler. *Reaction–Diffusion Equations and Their Application on Bacterial Communication*. 01 2017.

[42] M. Kwasnicki. Ten equivalent definitions of the fractional laplace operator. *Fractional Calculus and Applied Analysis*, 20:51–7, 2017.

[43] Mauricio Labadie and Anna Marciniak-Czochra. A reaction-diffusion model for viral infection and immune response. 05 2011.

[44] Assaely Leon and Guillermo Chacón-Acosta. Full finite element scheme for reaction-diffusion systems on embedded curved surfaces in r^3. *Advances in Mathematical Physics*, 2021:1–16, 04 2021.

[45] Jingtang Ma and Yingjun Jiang. Moving collocation methods for time fractional differential equations and simulation of blowup. *Science China Mathematics*, 54, 03 2011.

[46] Robert Marlow. Moving mesh methods for solving parabolic partial differential equations. 09 2010.

[47] Tamás Mona, István Lagzi, and Ágnes Havasi. Solving reaction-diffusion and advection problems with richardson extrapolation. *Journal of Chemistry*, 2015:9, 04 2015.

[48] James D. Murray. *Mathematical Biology I. An Introduction*, volume 17 of *Interdisciplinary Applied Mathematics*. Springer, New York, 3 edition, 2002.

[49] T. Nakagawa. Blowing up of a finite difference solution to $u_t = u_{xx} + u^2$. *Applied Mathematics and Optimization*, 2:337–350, 1975.

[50] Michael Neubert and Hal Caswell. Demography and dispersal: Calculation and sensitivity analysis of invasion speed for structured populations. *Ecology*, 81:1613–1628, 06 2000.

[51] J. L. Padgett, E. G. Kostadinova, C. D. Liaw, K. Busse, L. S. Matthews, and T. W. Hyde. Anomalous diffusion in one-dimensional disordered systems: a discrete fractional Laplacian method. *Journal of Physics A Mathematical General*, 53(13):135205, April 2020.

[52] Weiqing Ren and Xiao-Ping Wang. An Iterative Grid Redistribution Method for Singular Problems in Multiple Dimensions. *Journal of Computational Physics*, 159(2):246–273, April 2000.

[53] Marcel Riesz. Integrales de riemann-liouville et potentiels. 1988.

[54] Fei Shi, Wenguang Cheng, Mao Jinjin, and Tian-Zhou Xu. Blow-up and global existence of solutions for the time fractional reaction-diffusion equation. *Mathematics*, 9, 12 2021.

[55] S. Sugitani. On nonexistence of global solutions for some nonlinear integral equations. *Osaka Journal of Mathematics*, 12:45–51, 1975.

[56] Vicente Vergara and Rico Zacher. Optimal decay estimates for time-fractional and other nonlocal subdiffusion equations via energy methods. *SIAM Journal on Mathematical Analysis*, 47, 10 2013.

[57] Vicente Vergara and Rico Zacher. Stability, instability, and blowup for time fractional and other non-local in time semilinear subdiffusion equations. *Journal of Evolution Equations*, 17, 03 2017.